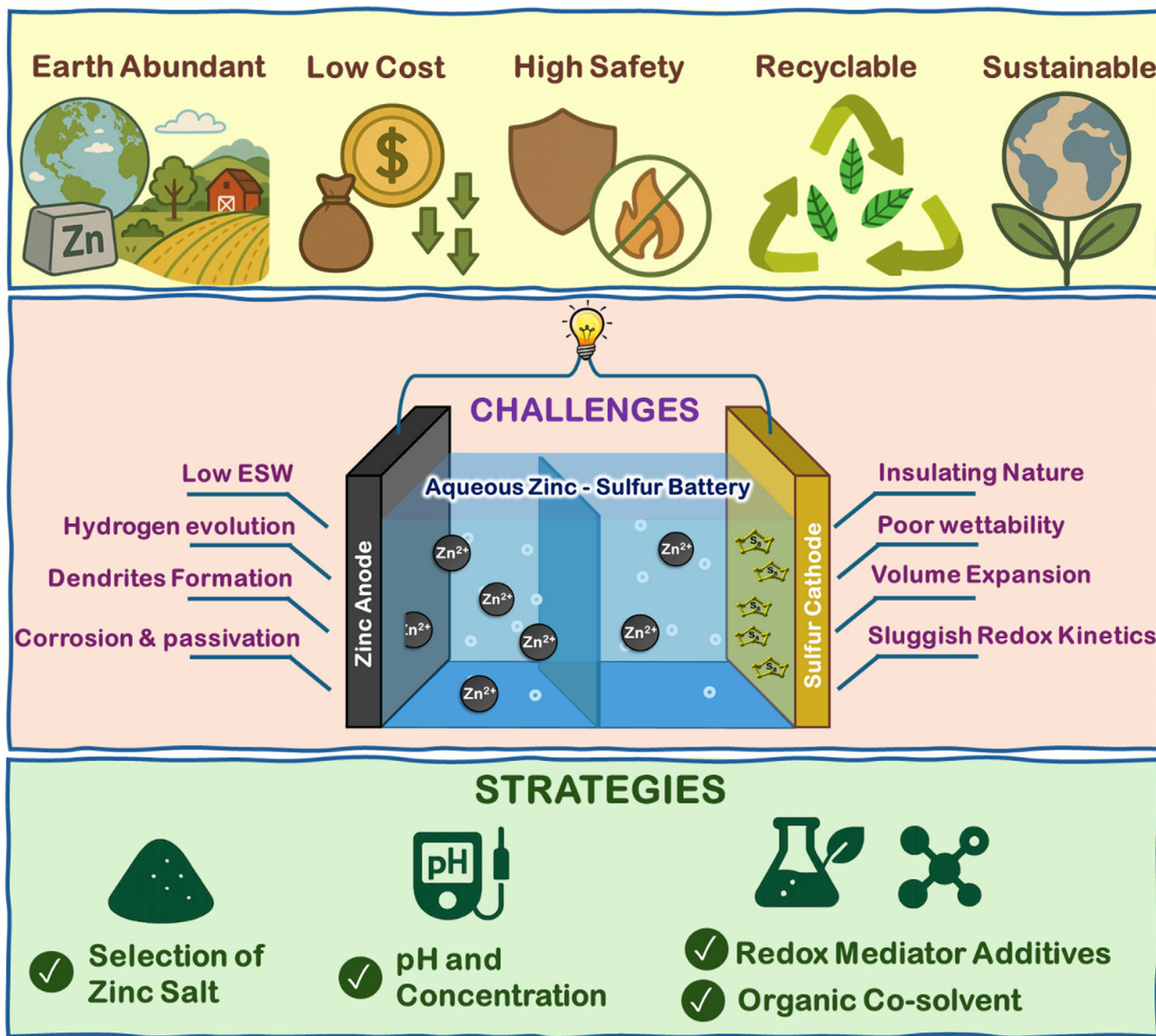


Advancements in Electrolytes for Aqueous Zinc–Sulfur Batteries: A Review

Srishti Kamboj, Dinesh Patel, and Ashwini Kumar Sharma*



Aqueous Zn–S batteries (AZSBs) have emerged as a next-generation energy storage system, offering high energy density, cost-effectiveness, and enhanced safety. However, their widespread adoption is restricted by multiple challenges, including sluggish sulfur redox kinetics that lead to high polarization voltage and poor capacity retention of the sulfur cathode. Moreover, unwanted reactions and irregular zinc dendrite development on the anode severely compromise electrochemical performance, particularly in capacity retention and cycle life. Among the various strategies, electrolyte engineering has emerged as an effective approach to overcoming these bottlenecks by regulating sulfur

conversion, stabilizing zinc plating/stripping, and expanding the electrochemical stability window. This review offers an in-depth exploration of recent innovations in electrolyte design for AZSBs, comprising discussions on the fundamental sulfur redox reaction mechanism, the challenges faced by AZSBs at both the cathode and anode, and the systematic strategies for enhancing battery performance through electrolyte modification. Finally, future research directions are proposed to optimize electrolyte formulations for achieving high-performance and long-lasting AZSBs, paving the way for their commercial viability.

1. Introduction

Rising concerns over pollution and climate change are driving a global transition toward cleaner energy alternatives, including wind and solar power.^[1] However, because of their intermittent and unpredictable nature, these renewable sources cannot be directly integrated with our electrical grid; rather, they require energy storage systems to balance energy supply and demand.^[2] Among various energy storage devices, lithium-ion batteries have arisen as a leading solution due to their high energy density, efficiency, and long cycle life.^[3] Nevertheless, limited availability of lithium resources, substantial costs, safety issues, and environmental impacts are valid concerns in the large-scale development of lithium-ion batteries. These concerns drive researchers to explore alternative energy storage technologies that are safer, more sustainable, and cost-effective.

In the exploration of alternative batteries, zinc metal has attracted significant attention owing to its high volumetric (5845 mAh cm^{-3}) and gravimetric capacity (820 mAh g^{-1}), low cost ($3 \text{ \$ kg}^{-1}$), high abundance (70 ppm in the crust of the earth), and environmental benignity.^[4,5] A major benefit of zinc over other metals is its electrochemical redox potential of -0.763 V (vs standard hydrogen electrode (SHE)), which is closer to the electrochemical stability range of water.^[6] As a result, Zn demonstrates compatibility and reversibility in aqueous media, rendering it a viable option for aqueous rechargeable batteries with enhanced safety and environmental sustainability. Hereby, the concept of aqueous zinc-ion batteries (AZIBs) has been developed where Zn is employed as an anode along with suitable cathode materials allowing (de)intercalation chemistry of zinc-ions. However, commonly used cathode materials in AZIBs, including Prussian blue analogs,^[7] organic compounds,^[8] manganese,^[9] and vanadium-based oxides,^[10] are unable to satisfy commercial requirements because of their low specific capacity and suboptimal energy density ($< 300 \text{ Wh kg}^{-1}$). Additionally, these materials struggle with structural instability caused by complex valence

and phase transitions during reactions, leading to self-corrosion and the dissolution of active materials.^[11] Considering these limitations of intercalation-based cathodes, it is imperative to explore conversion chemistry-based cathode materials that not only offer higher capacities but are also well-suited for aqueous systems.

Sulfur is a promising option in this regard due to its theoretical capacity (1675 mAh g^{-1}), rich abundance (0.03–0.1% in Earth's crust), low cost (\$150 per metric ton), and nontoxic nature. Indeed, sulfur has already been used as a conversion-based cathode in lithium–sulfur (Li–S) and sodium–sulfur (Na–S) battery systems, although typically with organic solvents such as 1,3-dioxolane (DOL), dimethoxyethane (DME), trimethylolpropane (TMP), etc.^[12–14] Utilizing sulfur, these batteries offer significantly higher energy density compared to the popular Li-ion batteries. However, they continue to rely on flammable organic electrolytes, raising serious safety concerns not only during operation but also throughout manufacturing and disposal. Due to the chemical reactivity and flammability of these nonaqueous systems, stringent handling protocols and specialized disposal measures are required. Moreover, their sensitivity to air and moisture necessitates energy-intensive manufacturing processes. Beyond these safety and processing challenges, Li–S and Na–S batteries also suffer from the dissolution and migration of intermediate polysulfide species (Li_2S_n or Na_2S_n , where $4 \leq n \leq 8$) into the electrolyte.^[15] This polysulfide shuttling results in the irreversible loss of active material, causing rapid capacity fading and poor cycling stability, key barriers to their practical application.^[16–18] In this regard, the emergence of aqueous zinc–sulfur batteries (AZSBs) offers a promising alternative. By replacing flammable organic electrolytes with safer, water-based systems, AZSBs address major safety and environmental concerns. Further, the zinc–sulfur chemistry inherently rules out polysulfide shuttling due to its one-step solid-to-solid conversion between S_8 and ZnS .^[19] Overall, the use of zinc—a low-cost, abundant, and non-toxic metal—combined with sulfur enables a sustainable and scalable energy storage solution in the form of AZSBs.

The concept of an AZSB was initially introduced by Bendikov et al. in 2002, where they demonstrated the innate potential of aqueous Zn–S chemistry along with foundational thermodynamic insights that energized subsequent research in the field.^[20] Despite this successful demonstration, the progress in AZSB

S. Kamboj, D. Patel, A. K. Sharma

Department of Chemical Engineering
Indian Institute of Technology Roorkee
Roorkee, Uttarakhand 247667, India
E-mail: ashwini@ch.iitr.ac.in

stalled for the next two decades due to the limited rechargeability of the system caused by the formation of insoluble and irreversible ZnS on the cathode.^[21–24] A breakthrough study by Li et al. in 2020 reignited interest in AZSBs, where they developed a rechargeable AZSB by enabling reversible conversion from ZnS to S with iodine as a redox mediator in an aqueous electrolyte.^[21] Since then, research activity in the area of AZSBs has picked up significantly, and subsequently, advancements have been made by novel modifications on both cathode and electrolyte materials (Figure 1). For the cathode side, performance gains were achieved via the introduction of different conductive carbon host materials, including carbon nanotubes (CNT),^[21] CMK-3,^[25] hollow carbon spheres,^[26] and activated carbon.^[27] Further progress was witnessed with the use of single-atom cobalt catalysts embedded within carbon hosts, which effectively enhanced conductivity and mitigated volume expansion stress during cycling.^[28] In parallel, progress was made via electrolyte modifications as well. To improve the reversibility of both the sulfur cathode and Zn anode, Yang et al. in 2022 introduced an organic cosolvent (in the form of tetraglyme) along with a redox mediator additive (in the form of I₂).^[26] In the same year, Zhou et al. introduced PEG-400 as a cosolvent, which effectively improved the reversibility of ZnS at the cathode and provided high stability of the Zn anode.^[29] Most recently, a transformative discovery revealed that carefully tailored electrolyte environments could induce a multistep sulfur conversion mechanism involving soluble polysulfide intermediates.^[22,30] This shift from a conventional solid–solid reaction pathway to a multistep process effectively enhanced the reversibility of sulfur redox chemistry. These advances have enabled AZSBs to achieve energy densities of 300–800 Wh kg⁻¹, substantially higher than those typically observed in AZIBs, which offer around 50–200 Wh kg⁻¹.^[30–32] Among different components of AZSB, the electrolyte serves as a critical component in governing both stabilizing the zinc anode and improving sulfur cathode reaction kinetics, directly affecting battery performance. Therefore, developing a suitable, high-performance electrolyte is essential for advancing AZSB technology. While

existing reviews have broadly covered AZSBs, a comprehensive discussion on electrolyte modification strategies remains limited.^[19,33,34] Given its critical function in facilitating zinc ion transport and maintaining connectivity between the electrodes, the electrolyte must be carefully optimized to achieve high performance, energy efficiency, and long-term stability in the AZSB system.

Hereby, this review offers a comprehensive analysis of the working principle of AZSBs and the critical problems hindering their large-scale application. Specifically, it delves into key issues associated with the aqueous electrolyte, including its limited electrochemical stability window (ESW), the growth of zinc dendrites, and corrosion at the zinc anode side. In addition, the major challenges associated with sulfur cathodes, such as sluggish reaction kinetics and rapid capacity fading, are also thoroughly discussed. Aligned with the focus of this review, we systematically examine recent advancements in electrolyte design and modification for AZSBs. This includes the use of additives, cosolvents, hybrid electrolytes, and eutectic systems aimed at enhancing sulfur redox kinetics, mitigating zinc anode degradation, and expanding ESW. Finally, we discuss key challenges, recent advancements, and future outlooks in electrolyte development, offering insights into its pivotal role in enhancing the performance and longevity of AZSBs.

2. Mechanism of Aqueous Zinc–Sulfur Battery

The AZSBs design comprises of cathode made up of sulfur/carbon composite and pure zinc metal as anode, with zinc salt dissolved in water serving as the electrolyte. Figure 2 illustrates its operation principle, which is typically based on a solid–solid one-step conversion pathway. Upon discharge, zinc ions will be stripped from the Zn anode and migrate to the sulfur cathode through the electrolyte, where S gets reduced and integrated with Zn²⁺ ions at the positive electrode, leading to the generation of zinc sulfide (ZnS) as the final discharge product. While charging, the



Srishti Kamboj is currently pursuing a Ph.D. under the supervision of Professor Ashwini Kumar Sharma at the Indian Institute of Technology Roorkee (IIT Roorkee). Her research focuses on the electrode surface and electrolyte modification, along with electrode material synthesis for the development of aqueous metal-ion and metal-sulfur batteries.



Dinesh Patel is currently a Ph.D. student at the Indian Institute of Technology Roorkee (IIT Roorkee) under the supervision of Prof. Ashwini Kumar Sharma. His research interests lie in the cathodes and electrolyte design for aqueous rechargeable metal ion and metal sulfur batteries.



Ashwini Kumar Sharma is currently an Associate Professor in the Department of Chemical Engineering at the Indian Institute of Technology Roorkee (IIT Roorkee). Before joining IIT Roorkee, he worked as an Assistant Professor at the Indian Institute of Technology Patna (IIT Patna), as a technical lead at the Samsung R&D Institute (Bangalore), and as a research fellow at the National University of Singapore (NUS). His research focuses on emerging electrochemical energy systems with regard to their system and component design challenges.

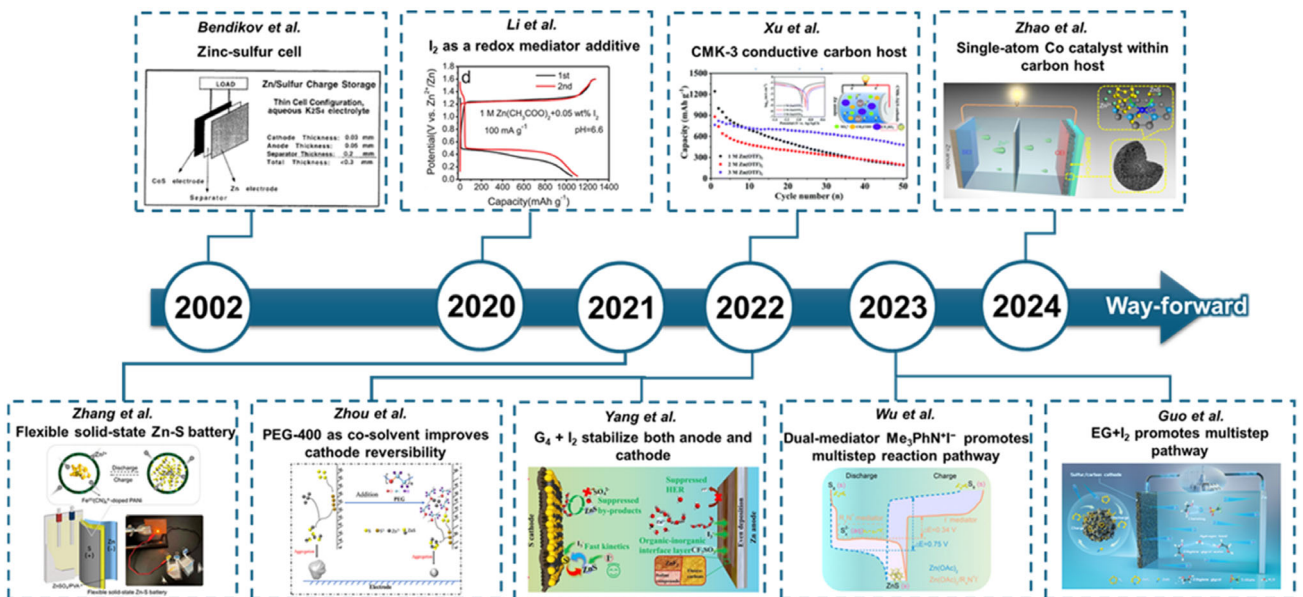


Figure 1. Historical development of aqueous zinc–sulfur batteries.

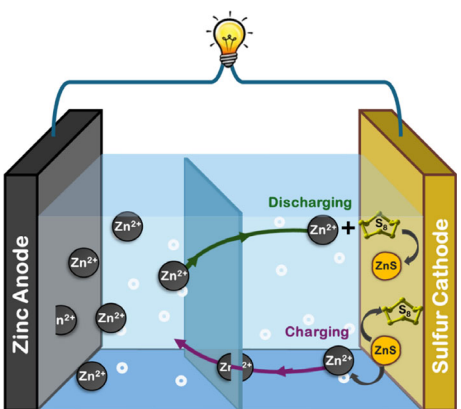


Figure 2. Working mechanism of the aqueous zinc-sulfur battery.

reaction gets reversed from ZnS to S . The full-cell reaction is proposed as



Various characterization techniques have been employed to illustrate the solid–solid conversion reaction mechanism of AZSBs. To precisely determine the phase transition during the conversion reaction, X-ray diffraction analysis was performed at different potentials. As shown in Figure 3a, the bare positive electrode exhibits characteristic diffraction peaks of elemental S at 23.1° . Upon discharging to point C, the emergence of a ZnS diffraction peak at 28.6° (111) coincides with the gradual decline in sulfur peak intensity, highlighting the progressive conversion of S to ZnS . At point D, the complete disappearance of sulfur peaks and the clear appearance of ZnS diffraction signals at 28.6° (111), 47.5° (220), and 56.3° (311) confirm complete ZnS

formation. During the subsequent charging process to point G, the sulfur peaks reappear, suggesting a reversible conversion of ZnS back to S .^[26] This is further supported by Raman spectroscopy, which reveals no polysulfides or intermediate species formation throughout the reaction (Figure 3b).^[26] At point D (full discharge), various Raman peaks of ZnS are observed at 182 , 316 , 371 , and 423 cm^{-1} , while sulfur-related peaks at 218 and 475 cm^{-1} diminish, confirming ZnS formation. Upon recharging to point G, the ZnS peaks diminish, and sulfur peaks at 218 and 475 cm^{-1} reappear, indicating the solid–solid conversion of ZnS to S . The valence-state evolution of the sulfur cathode is revealed by X-ray photoelectron spectroscopy (XPS) analysis (Figure 3c). The pristine S 2p spectrum shows doublets at 164.0 and 165.2 eV , corresponding to S . Upon discharging to point B, peaks at 161.7 and 163.0 eV confirm the formation of ZnS . At point C, the S peaks disappear, verifying ZnS as the final discharge product. At points D to F (during recharging), the S peaks reappear, indicating a reversible S-ZnS conversion throughout cycling.^[35] The formation of ZnS is confirmed by its interlayer spacing of 0.314 nm , which aligns well with the lattice plane (111) of ZnS (Figure 3d). Additionally, the elemental mapping of Zn and S further validates ZnS as the dominant discharge product (Figure 3e).^[21] These characterizations provide evidence that the S redox process follows solid–solid conversion pathway without any intermediates in AZSBs.^[21] However, recent studies on AZSBs also revealed the multistep conversion pathway in the hybrid electrolyte to accelerate the redox kinetics.^[22,30]

3. Challenges due to Aqueous Electrolyte

The advancement of AZSBs is hindered by several critical challenges that must be addressed to enhance their efficiency,

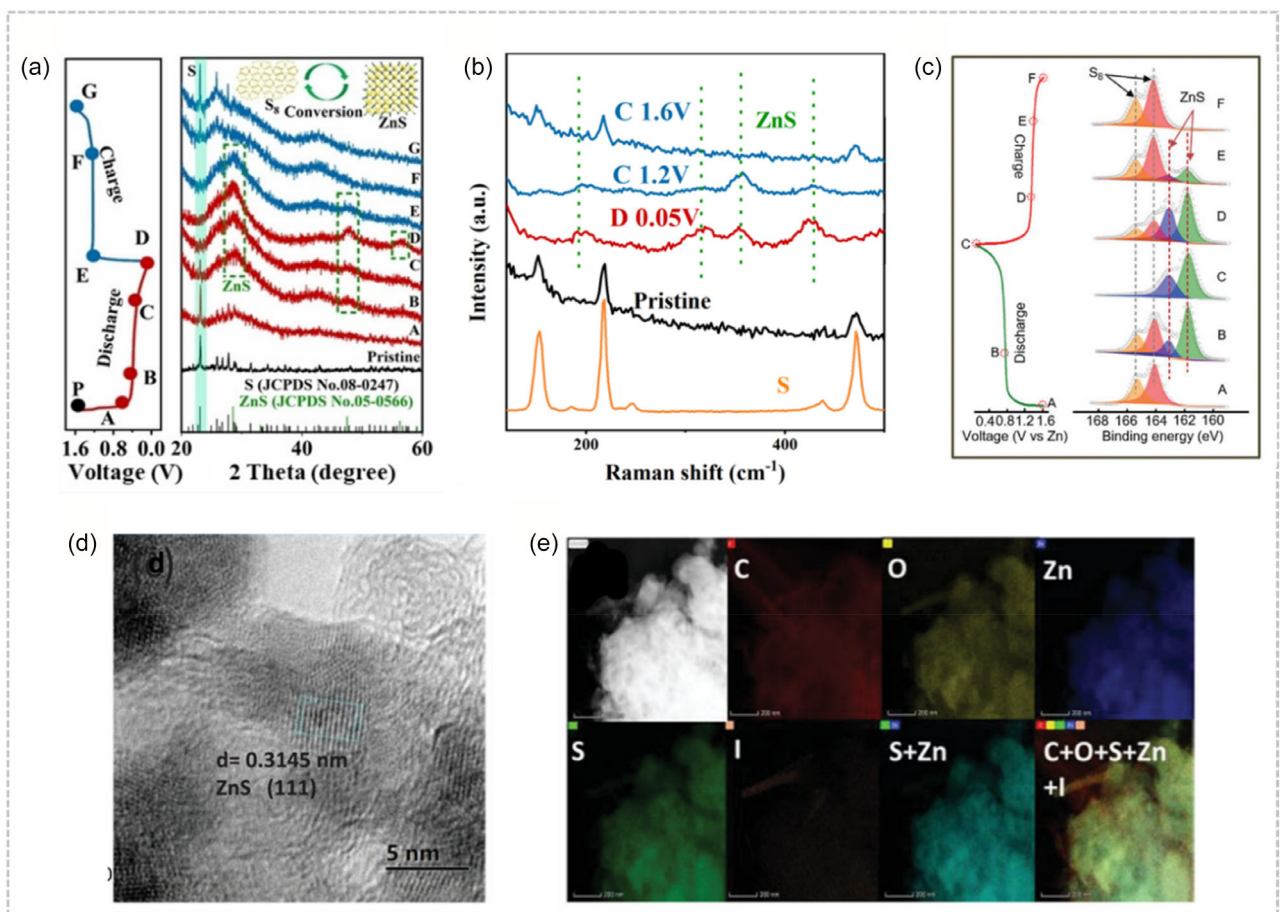


Figure 3. a) XRD patterns of the cathode of AZSB shown at different charging and discharging potential on the left side. b) Raman spectra of the S cathode at different charging and discharging potential. This panel was reproduced with permission.^[26] Copyright 2022 Wiley. c) XPS analysis of sulfur cathode after discharge and charge to specific states. This panel was reproduced with permission.^[35] Copyright 2023 Wiley. d) TEM image showing fully discharged cathode of AZSB and e) corresponding TEM mapping. This panel was reproduced with permission.^[21] Copyright 2020 Wiley.

long-term stability, and overall performance. This section explores the key obstacles that impact the viability of AZSBs, including the restricted ESW, zinc dendrite formation, Zn anode corrosion and passivation, poor sulfur cathode kinetics, and capacity degradation of the sulfur cathode (Figure 4).

3.1. Electrolyte Stability Window

ESW defines the potential range over which an electrolyte maintains stability, without undergoing decomposition and triggering parasitic side reactions.^[36] One of the fundamental challenges in aqueous batteries is their inherently narrow ESW, typically limited to 1.23 V. Beyond this range, water electrolysis takes place, resulting in the evolution of hydrogen and oxygen gases, which not only deplete the electrolyte but also cause gas generation and battery swelling.^[37] As a result, the limited ESW directly restricts the maximum achievable voltage of aqueous batteries, posing a significant barrier to their energy output.^[38]

During charging, the desired reaction at the zinc electrode is zinc deposition, where Zn^{2+} gains two electrons to form metallic Zn. However, the hydrogen evolution reaction (HER) is an unavoidable parasitic reaction because the reduction potential of HER is higher than that of Zn^{2+}/Zn (-0.76 V vs SHE) at all pH ranges, making HER thermodynamically favorable over the zinc deposition. The Nernst equation shows that the reduction potential associated with the HER in an aqueous medium is given by $E_{HER} = -0.0592 \times pH$, indicating HER is strongly pH dependent. While pH does not alter the ESW, it only affects the

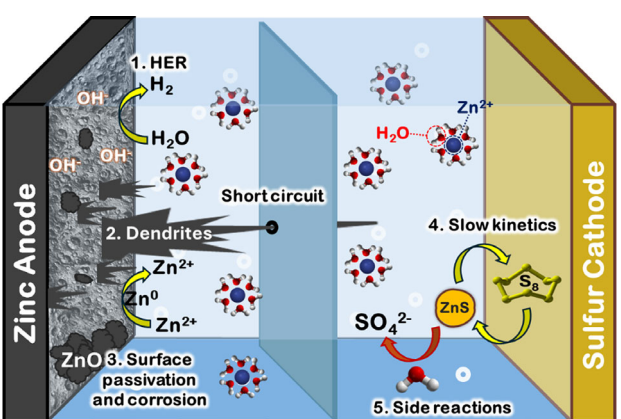


Figure 4. The schematic illustrates the critical challenges in aqueous Zn–S batteries.

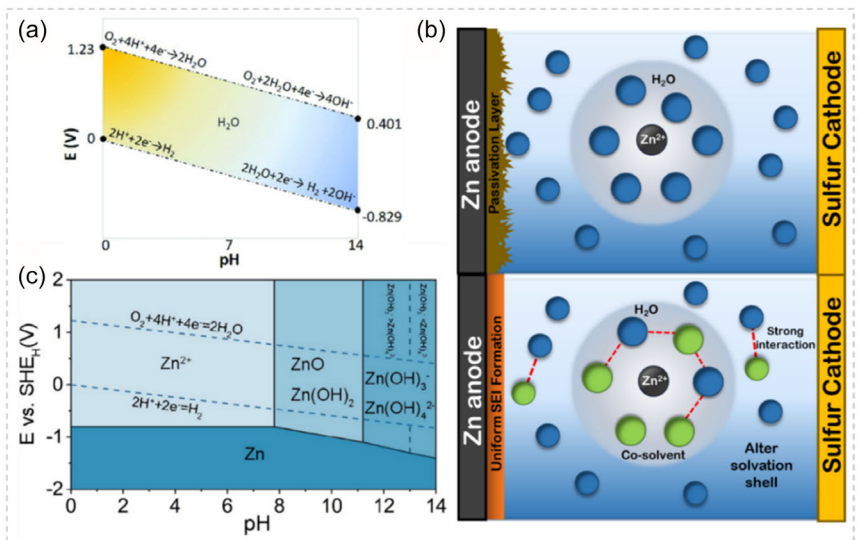


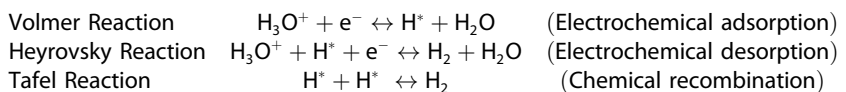
Figure 5. a) Pourbaix diagram of H₂O. This panel was reproduced with permission.^[117] Copyright 2021 Royal Society of Chemistry. b) Zn²⁺ solvation structure in bare aqueous (up) and modified aqueous electrolyte (down). c) Relation between potential and pH of Zn metal in aqueous media (Pourbaix diagram). This panel was reproduced with permission.^[56] Copyright 2023 Royal Society of Chemistry.

potentials of HER (Figure 5a).^[39–41] The overall reaction pathway of HER, depending on pH, is as follows.

In neutral and basic electrolytes:



In acidic electrolytes:



Since HER consumes electrons that would otherwise contribute to zinc deposition, it leads to lower coulombic efficiency (CE). In this context, broadening the ESW and suppressing HER are crucial for achieving high-voltage and efficient AZSBs.^[43] This can be achieved by lowering the free H₂O content and its activity in the electrolyte, modifying the zinc ion solvation structure, and forming a solid electrolyte interface using methods like water-in-salt electrolytes, pH control, and adding organic cosolvents.^[44,45] To better understand the changes in solvation structure, a representative example of cosolvent incorporation in an aqueous electrolyte is depicted in Figure 5b. In the bare aqueous electrolyte, the Zn²⁺ solvation sheath is dominated by H₂O molecules. When an organic cosolvent is introduced, it modifies the solvation structure by participating in the Zn²⁺ solvation via coordination and hydrogen-bond interactions.^[46,47] This phenomenon was investigated through molecular dynamics (MD) simulations, where radial distribution function (RDF) and coordination number (CN) analyses confirmed the displacement of HO molecules by organic solvent molecules around Zn²⁺ ions.^[22,48–50] During Zn

HER occurs through multiple electrochemical steps at the zinc-electrolyte interface. The process begins with the Volmer reaction, where hydronium ions (H₃O⁺) are discharged to form hydrogen atoms, which are absorbed on the zinc surface. Then, another hydronium ion reacts with the already adsorbed hydrogen atom (H*) on the zinc surface to produce molecular hydrogen (H₂) through the Heyrovsky reaction. Alternatively, the two adsorbed hydrogen atoms can also combine to form hydrogen gas, known as the Tafel reaction.^[42]

deposition, the cosolvent undergoes reductive decomposition, resulting in the formation of the SEI layer that effectively suppresses side reactions, including HER.

3.2. Zinc Dendrite Formation

During the initial charging, Zn²⁺ ions move toward the zinc anode under the applied electric field and get deposited as a random cluster on its surface. This deposition begins with a 2D diffusion process, known as the nucleation step, where uniformity is strongly influenced by the electrolyte composition and ion transport properties.^[51] As Zn²⁺ plating continues, the Zn²⁺ ions preferentially deposit on the most favorable charge transfer site with a lower activation barrier. Since Zn²⁺ requires less nucleation energy in this growth phase, deposition occurs on existing clusters, which often leads to nonuniformity at the anode surface. The selection of electrolyte plays a pivotal role in controlling this Zn deposition behavior. Electrolytes with poorly coordinated Zn²⁺

solvation structures or high ionic resistance can promote localized ion accumulation, exacerbating uneven Zn plating. Additionally, the presence of free H₂O molecules in aqueous electrolytes promotes parasitic reactions like hydrogen evolution, further influencing zinc deposition dynamics.^[52,53]

The nonuniform Zn plating gives rise to structural defects such as crystal tips, grain boundaries, and dislocations, eventually inducing dendrite growth. Over time, these dendrites can pierce the separator, causing an internal short circuit and failure of the battery.^[54] Furthermore, during prolonged cycling, the detachment of elongated Zn dendrites results in the generation of inactive "dead Zn," which migrates to the vicinity of the zinc anode. This process consumes active material and leads to irreversible capacity loss. To mitigate these challenges, electrolyte modification strategies, such as introducing additives, using highly concentrated electrolytes, or employing hybrid solvent systems, have been explored to regulate Zn²⁺ solvation, suppress dendrite formation, and enhance electrochemical stability.^[55]

3.3. Zinc Corrosion and Passivation

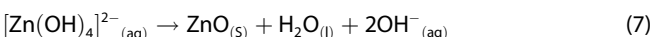
The direct exposure of the Zn metal to the electrolyte causes corrosion and generates a passivation layer from reaction byproducts, posing significant challenges in aqueous zinc-based batteries (AZBs). These processes contribute to increased self-discharge and significantly lower CE of the zinc-based battery. As shown in Figure 5c, the corrosion behavior of zinc strongly depends upon the pH value of the aqueous electrolyte.^[56] In strongly acidic conditions (pH < 4.0), zinc is readily oxidized, resulting in excessive Zn²⁺ loss from the anode into the electrolyte. Simultaneously, a vigorous HER takes place, producing hydrogen gas bubbles that compromise the contact stability between cell components, ultimately resulting in cell failure. In contrast, mildly acidic conditions appear to reduce HER. However, the ongoing consumption of protons leads to the formation of hydroxide ions (OH⁻), causing a gradual increase in the local pH near the zinc surface. The generated OH⁻ ions interact with dissolved zinc ions in the electrolyte to form inert byproducts such as, ZnSO₄(OH)₆·xH₂O or Zn₄ClO₄(OH)₇. These compounds precipitate and deposit on the zinc surface as a passivation layer, which increases internal resistance and hinders Zn²⁺ ion transport kinetics.^[57-59]

In basic conditions, Zn²⁺ ions interact with hydroxide ions (OH⁻) to form different zinc species depending on the OH⁻ concentration.^[60,61] At moderate OH⁻ levels or in slightly basic medium, Zn²⁺ reacts with hydroxide ions to form zinc hydroxide (Zn(OH)₂), which precipitates as a white solid. In strongly alkaline environments with excess OH⁻ (pH > 11), Zn²⁺ further coordinates with 4OH⁻ and gets stabilized as zincate complexes, [Zn(OH)₄]²⁻. During charging, these zincate complexes eventually precipitate as ZnO, forming a thick, insulating layer on the zinc surface. This passivation layer promotes corrosion, blocks active sites, and consequently degrades the rechargeability and overall performance of the zinc battery.^[53,62,63]

When pH > 8:



When pH > 11:



Thus, both alkaline and acidic environments introduce severe side reactions and passivation effects that compromise the stability of zinc plating/stripping.^[64] In contrast, maintaining a neutral to mildly acidic condition (pH≈4 to 6) limits the passivation effects comparatively and thus, improves the cyclability of zinc metal to some extent. Consequently, mildly acidic Zn salts dissolved in H₂O, such as ZnCl₂, ZnSO₄, and Zn(CF₃SO₃)₂, are commonly employed as electrolytes in AZSBs to provide a favorable pH environment. Further modification of the Zn metal surface through artificial coatings or the grafting of functional groups can significantly reduce Zn corrosion and surface passivation.

3.4. Poor Sulfur Cathode Kinetics

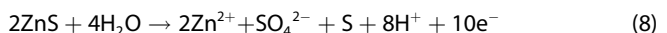
Although sulfur-based cathodes offer high theoretical capacity, their application in AZSBs is significantly hindered by the sluggish solid-solid conversion kinetics and poor electrical conductivity. The primary challenge arises from the insulating nature of both elemental sulfur ($S_8 \approx 5 \times 10^{-28} \text{ S m}^{-1}$) and zinc sulfide ($\text{ZnS} \approx 10^{-9} \text{ S m}^{-1}$), which severely hinders electron conduction and zinc ion transport.^[65,66] This low conductivity leads to the accumulation of ZnS on the cathode surface, further impeding the reversibility of the sulfur redox process during charging. Also, ZnS exhibits a strong binding energy (237.73 kJ mol⁻¹) and low solubility ($K_{\text{sp}} = 1.2 \times 10^{-23}$) in aqueous electrolytes, further imparting difficulty to its reverse conversion to sulfur.^[22] Overall, low conductivity and high binding energy of ZnS restrict the charge transfer and cause sluggish reaction kinetics, thereby limiting the overall efficiency of the battery.^[67]

Additionally, the hydrophobic nature of sulfur results in poor wettability towards the water-based electrolyte.^[68] This lack of interfacial contact increases the energy barrier for Zn²⁺ ion diffusion, further contributing to sluggish conversion kinetics and substantial polarization during charge-discharge cycles.^[69] Addressing these challenges requires electrolyte engineering, where researchers have explored the use of various redox mediators to accelerate reaction kinetics and organic cosolvents to enhance the sulfur cathode wettability and improve interfacial compatibility. Moreover, tailored electrolyte formulations can modify the solvation sheath of Zn²⁺, thereby enhancing electrolyte stability and mitigating sulfur-related side reactions.

3.5. Capacity Degradation of Sulfur Cathode

Various unwanted reactions occur when the sulfur cathode interacts with aqueous electrolyte, leading to poor capacity retention

in AZSBs. During charging, the discharge product ZnS dissociates and undergoes oxidation, ultimately forming elemental sulfur. However, a fraction of the S^{2-} anions from ZnS undergo over-oxidation, forming irreversible byproducts such as sulfate anions (SO_4^{2-}) in aqueous media. This over-oxidation of ZnS prevents the complete utilization of active material due to sulfur loss, which leads to long-term capacity fading.^[21] The degradation pathway can be expressed as



In acidic media, loss of sulfur species is further influenced by the unstable nature of ZnS, which undergoes disproportionation reactions under low pH conditions, producing soluble hydrogen sulfide species such as, bisulfide ions (HS^-) or hydrogen sulfide gas (H_2S). The continuous depletion of sulfur active material reduces the electrochemical capacity over repeated charge-discharge cycles, leading to poor capacity retention and cycle life. Additionally, the evolution of H_2S gas can cause further side reactions and safety concerns.^[22]

4. Strategies for Improvement

As we discussed in the previous section, the long-term viability of AZSBs is hindered by several challenges, including poor sulfur redox reaction kinetics, zinc dendrite formation, HER, and electrode passivation. These issues largely stem from undesirable side reactions and inefficient ion transport, both of which are closely linked to electrolyte composition and solvation behavior. Upon dissolution, zinc salts form solvated zinc ions, typically in the form of $[\text{Zn}(\text{H}_2\text{O})_6]^{2+}$. The solvation environment, including the strength of ion-water interactions and the nature of the anions, significantly affects electrolyte stability and electrochemical performance.^[46,70] To address the aforementioned challenges, researchers have explored diverse electrolyte engineering strategies, including zinc salt optimization, concentration and pH tuning, incorporation of redox mediators, functional additives and cosolvents, development of hybrid electrolytes, introduction of eutectic electrolyte, and solid-state/hydrogel electrolyte systems. The various strategies adopted by different researchers are summarized in Figure 6 and explained as below.

4.1. Selection of Zinc Salt

The first and foremost decision with regard to electrolyte preparation is certainly the right selection of solvent and salt. Concerning aqueous batteries, the solvent is fixed as water, so the focus naturally shifts to the selection of the salt. In the earlier research on AZSBs, ZnSO_4 has been the most used electrolyte salt due to its aqueous solubility, cost-effectiveness, and stability. However, it suffers from the accumulation of a passive layer on the zinc anode, consisting of inert byproducts such as $\text{Zn}_4(\text{OH})_6\text{SO}_4 \cdot 5\text{H}_2\text{O}$.^[71] This side reaction not only depletes the electrolyte but also reduces CE and increases interfacial

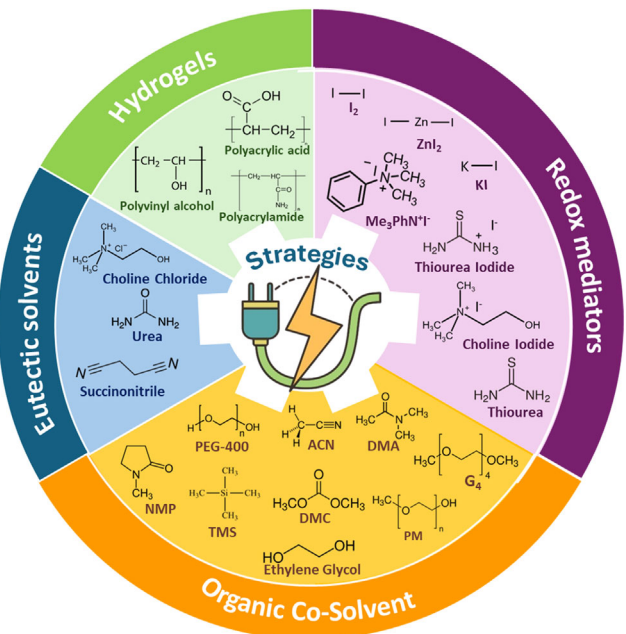


Figure 6. Electrolyte design strategies for high-performance AZSBs.

resistance, thereby hindering ion transport. Therefore, several other water-soluble zinc-based salts, such as, ZnCl_2 , $\text{Zn}(\text{ClO}_4)_2$, $\text{Zn}(\text{CH}_3\text{COO})_2$, $\text{Zn}(\text{CF}_3\text{SO}_3)_2$, $\text{Zn}(\text{TFSI})_2$, and ZnBr_2 are being explored for improved performance.^[72-77] Selection of zinc salts with bulky anions, particularly those with electron-withdrawing groups, can promote dissociation and improve cation transport. Notably, $\text{Zn}(\text{CF}_3\text{SO}_3)_2$ has gained attention due to its large CF_3SO_3^- anions, which effectively alter the Zn^{2+} solvation shell structure.^[25] This modification reduces the H_2O molecules in the Zn^{2+} solvation structure, thereby inhibiting the solvation effect and suppressing HER and corrosion at the zinc anode. As a result, $\text{Zn}(\text{CF}_3\text{SO}_3)_2$ exhibits higher ionic conductivity, enabling faster Zn^{2+} transport kinetics and enhanced cycling stability. Besides the size of anions, the donor number of anions can serve as another criterion for selecting zinc salts. The donor number of anion positively affects both the extent of salt dissociation and the solubility of sulfide species in the electrolyte. The latter is particularly important from the cathode perspective, as the solubility of ZnS affects its growth behavior, determining whether ZnS deposits as a porous 3D structure on the carbon substrate or forms a dense 2D passivation layer. In this regard, ZnBr_2 is a promising salt for preparing AZSB electrolytes because of the higher donor number of bromide anions.^[78] Higher sulfide solubility, as observed with ZnBr_2 , promotes 3D ZnS growth, expanding active sites and maintaining the electronic conductivity in the cathode. Conversely, $\text{Zn}(\text{TFSI})_2$, with a lower donor number (DN), results in a dense 2D ZnS layer, which limits the charge transport and overall electrochemical performance. In summary, selecting an optimal zinc salt with a suitable counter anion is essential for suppressing the parasitic reactions at the anode and exhibiting a favorable growth morphology of ZnS at the cathode.

4.2. Tuning pH and Concentration of the Salt

Once salt is finalized, its concentration and pH of the electrolyte are two important parameters determining the performance of the final electrochemical cell. High-concentration electrolytes effectively alter the Zn^{2+} ion solvation structure by lowering the free H_2O molecules.^[79] This suppression of water activity mitigates parasitic reactions such as HER and electrolyte decomposition, thereby enhancing the electrode–electrolyte interfacial stability, inhibiting the zinc dendrites growth, and prolonging cycling performance. For example, in an AZSB, increasing the concentration of $Zn(CF_3SO_3)_2$ with 0.1 wt% I_2 effectively suppresses the HER at the Zn anode, implying a wider ESW and preventing Zn anode corrosion.^[25] This enhances the battery performance, allowing it to consistently retain a capacity of 270 mAh g^{-1} over 100 cycles at 1 A g^{-1} , showcasing its durability.

Beyond salt concentration, another critical parameter is maintaining electrolyte pH within an optimal range. As described earlier, pH is a key parameter controlling the HER, corrosion, and passivation at the negative electrode and the disproportionation of ZnS at the positive electrode. The electrochemical behavior of the S-based cathode is studied for three readily available electrolytes of different pH values.^[21] In 1 M $Zn(CF_3SO_3)_2$ (pH = 4.4), S@CNTs-50 exhibited an initial CE of 63%, accompanied by a high voltage hysteresis of 1.1 V, indicating poor reaction kinetics. When tested in 1 M $ZnSO_4$ (pH = 5.2), the initial CE further declined to 26% due to increased parasitic side reactions, though the voltage hysteresis slightly improved to 0.95 V, suggesting marginally enhanced reaction kinetics. In contrast, in 1 M $Zn(CH_3COO)_2$ (pH = 6.5), the initial CE significantly increased to 98%, with a reduced voltage hysteresis of 0.9 V, implying improved reaction kinetics as well as better suppression of parasitic reactions. These findings highlight the critical role of electrolyte pH in enhancing CE, minimizing voltage hysteresis, and ensuring stable Zn–S battery operation. Although the effects of pH and anion chemistry are intertwined in this study, the observed trends—such as reduced CE at lower pH—suggest that acidic conditions promote side reactions and accelerate sulfur loss, thereby contributing to capacity degradation. The role of pH in zinc electrochemistry and associated side reactions is well documented,^[80,81] however, AZSB-specific studies that examine pH as an isolated variable are still lacking. There is a need for systematic investigations where pH is independently controlled—using buffers or titration—while keeping the salt composition constant, to clearly understand its effect on reaction kinetics, sulfur stability, and surface passivation.

4.3. Aqueous-Dominant Electrolytes with Redox Mediator Additives

In the search for an ideal electrolyte, optimizing the pH and salt concentration can enhance battery performance to some extent, but these enhancements do not fully resolve the challenges faced by AZSBs. So, it becomes essential to introduce additional components or additives into the electrolyte to further address these

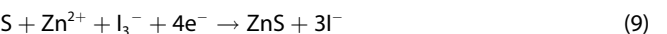
issues. Highlighting one of the major challenges faced by AZSBs is the sluggish sulfur redox conversion kinetics from ZnS to S, which significantly limits the overall battery efficiency. To tackle this, redox mediators can be employed as electrolyte additives, offering a promising approach to accelerate the slow kinetics of the sulfur cathode.^[67,82] These redox-active electrolyte additives participate in reversible redox reactions by acting as electron transfer facilitators. Thus, they reduce the energy barrier and ease the ZnS to S conversion, lowering the voltage polarization in the cell.

To enhance the reaction kinetics and achieve high capacity, redox mediators must satisfy the following key criteria: 1) they should exhibit fast and reversible electron transfer; 2) their electrochemical redox potential should be close to the thermodynamic equilibrium potential of the AZSBs; 3) they should possess high solubility in electrolyte; and 4) they must show good electrochemical stability during operation.^[83] This section focuses on discussing the usage of both inorganic (e.g. iodide), and organic (e.g. thiourea) based redox mediators, which predominantly meet the above requirements to serve as potential redox mediators for AZSBs.^[21,84,84]

4.3.1. Iodine-Based

Recently, I_2 has emerged as a promising agent to catalyze sulfur redox reactions. It effectively enhances the sulfur redox kinetics by lowering the reaction barriers.^[21] With the promise of enhanced reaction kinetics at the cathode, iodine has also been applied as a redox mediator in AZSBs as well. In AZSBs, it was suggested that the I_3^-/I^- redox couple involves a four-electron transfer process, which enhances the solid–solid conversion catalytic mechanism at the sulfur cathode.^[85,86] The reaction pathway can be summarized as follows.

Discharge process:



Charge process:



During discharge, initially iodine (I_2) is reduced to iodide ions (I^-) by accepting electrons. The generated I^- then reacts with neutral I_2 molecules to form triiodide ions (I_3^-), where I_3^- species can facilitate the reduction of sulfur. Meanwhile, ZnS particles tend to interact strongly with I^- , leading to atomic rearrangement within the ZnS structure. This interaction weakens the Zn–S bonds, introduces lattice defects, and promotes the cleavage of Zn–S bonds, thus enabling the reversible conversion of ZnS.

Recent studies have explored different forms of iodine-based mediators, ranging from molecular I_2 to various iodide-based salts, to optimize redox activity and battery performance. In the following, we provide a detailed discussion of these approaches, highlighting their distinct roles and effects within the redox mediation process.

4.3.1.1. Molecular Iodine (I_2)

Jiang et al. (2020) published a pioneering work by introducing nonpolar iodine (I_2) as a redox mediator additive to promote the reversible sulfur conversion reaction in AZSBs.^[21] For a comparative assessment, they fabricated AZSB coin cells using 1 M $Zn(CH_3COO)_2$ with and without the addition of iodine. The cell with bare electrolyte delivered a reversible specific capacity of 685 $mAh\ g^{-1}$, which significantly improved to 1105 $mAh\ g^{-1}$ (at 100 $mA\ g^{-1}$) when 0.05 wt% I_2 is added in the electrolyte. Not only the increased capacity, but the cell with modified electrolyte also featured a stable 0.5 V discharge plateau and a reduced voltage hysteresis of 0.72 V, indicating improved Zn^{2+} ion kinetics (Figure 7a,b).

However, the nonpolar iodine (I_2) shows poor solubility in water (typically 0.05–0.1 wt%), which leads to the formation of insufficient catalytic I^- for the reversible ZnS-to-sulfur conversion during charging.^[31,87] Therefore, researchers have investigated various iodide (I^-) salts, which offer higher water solubility than I_2 , for example, zinc iodide (ZnI_2), potassium iodide (KI), ammonium iodide, etc. These salts can provide sufficient I^- , which can effectively lower the energy barrier for the interconversion of sulfur and ZnS and thus improve the sulfur cathode kinetics.

4.3.1.2. Zinc Iodide (ZnI_2)

While searching for an alternative redox mediator to molecular iodine, Peng et al. investigated the potential of highly water-soluble ZnI_2 , which releases a sufficient amount of I^- ions when introduced into the aqueous electrolyte.^[31] The released I^- ions effectively facilitate the conversion of ZnS back to elemental sulfur, thus enhancing the conversion kinetics of the sulfur redox reactions (Figure 7c,d). The researchers confirmed the redox mediation mechanism of I^- ions by performing electrochemical analysis and theoretical simulations. Density functional theory (DFT) revealed that I^- ions absorb on ZnS during charging, causing an upward shift in the d-band center of ZnS that leads to a strong interaction between I^- and ZnS. This triggers atomic rearrangements, including elongation of Zn–S bonds, which facilitates bond breaking and electro-oxidation of ZnS, ultimately enabling highly reversible ZnS to S conversion. To confirm the performance gains, a comparative study was done by assembling two devices, one using I_2 and the other using ZnI_2 . As shown in Figure 7e, both systems exhibit similar initial discharge profiles, but the ZnI_2 -based battery demonstrates much lower polarization during charging and delivers a high reversible capacity of 1725 $mAh\ g^{-1}$, nearly double that of the I_2 -based system (807 $mAh\ g^{-1}$). This enhanced reversibility leads to markedly better cycling stability, retaining 67% of its capacity after 50 cycles (1 $A\ g^{-1}$), in contrast to only 12% for I_2 (Figure 7f). These improvements are attributed to the continuous presence of catalytically active I^- species from ZnI_2 , which sustain efficient sulfur electro-oxidation throughout cycling.

4.3.1.3. Trimethylphenyl Ammonium Iodide ($Me_3PhN^+I^-$)

In the series of applications of iodine-based salts as redox mediators in AZSBs, Wu et al. designed a dual mediator system based on $Me_3PhN^+I^-$.^[30] The distinctive gain with this salt was the generation of soluble polysulfide intermediates at the sulfur cathode, which induces a multistep reaction mechanism to accelerate the redox kinetics (Figure 7g). The Me_3PhN^+ cation acts as a dissolution mediator by facilitating the initial ring-opening reduction of S_8 to S_8^{2-} , which undergoes chain cleavage to form shorter chain polysulfide intermediates (S_4^{2-}/S_6^{2-}) during discharge. Theoretical calculations reveal that this reaction proceeds more readily in the presence of Me_3PhN^+ due to a lower activation energy than Zn^{2+} . The resultant intermediates rapidly react with Zn^{2+} ions to form ZnS, transforming the sluggish solid–solid conversion into an efficient solid–liquid–solid pathway. In parallel, the iodide anion functions as a redox mediator, catalyzing ZnS oxidation to S via the I^-/I_3^- redox couple during charging. Interestingly, the solubility of I_3^- is also lowered by the presence of Me_3PhN^+ , preventing the polyiodide shuttling while retaining its catalytic ability. Overall, this approach significantly improved redox conversion kinetics at the sulfur cathode and helped to achieve a high specific capacity of 1659 $mAh\ g^{-1}$ (0.1 $A\ g^{-1}$) along with a low overpotential of 0.34 V (Figure 7h).

4.3.1.4. Iodinated Thiourea (TUI)

The effectiveness of iodine-based mediators in AZSBs was further demonstrated by Liu et al. when they introduced iodinated thiourea as an additive in the electrolyte.^[88] In their study, the incorporation of iodinated thiourea reduced the activation energy required for Zn extraction from crystalline ZnS to 1.26 V, resulting in a higher specific capacity of 503 $mAh\ g^{-1}$ in comparison to 216 $mAh\ g^{-1}$ for the bare electrolyte (Figure 7i). Traditional cyclic voltammetry (CV) analysis was used to discern the improvements with TUI additive (Figure 7j). In the absence of TUI, no clear cathodic peak was observed, indicating that ZnS oxidation does not occur below 1.4 V. In contrast, with TUI addition, a clear cathodic peak was observed at 1.2 V, indicating oxidation of both I^- and ZnS. With TUI, the CV curves exhibited three distinct reduction peaks, with the peak at 1.2 V attributed to the reduction of I_3^- , while the remaining two peaks were associated with the formation of ZnS.

4.3.1.5. Choline Iodide (CHI)

While iodine-based compounds were being explored for redox mediation purposes on the cathode, Zhao et al. found that choline iodide (CHI) as an electrolyte additive can manipulate the electrochemistry on both the sulfur cathode and zinc anode. DFT calculations were performed to determine the bandgap between the energy levels of different electrolyte components. The results showed that the Zn^{2+} –CHI complex exhibits the lowest HOMO–LUMO energy gap, indicating enhanced electron transfer ability at the complex interface. Thus, CHI, in the role of dual-functional

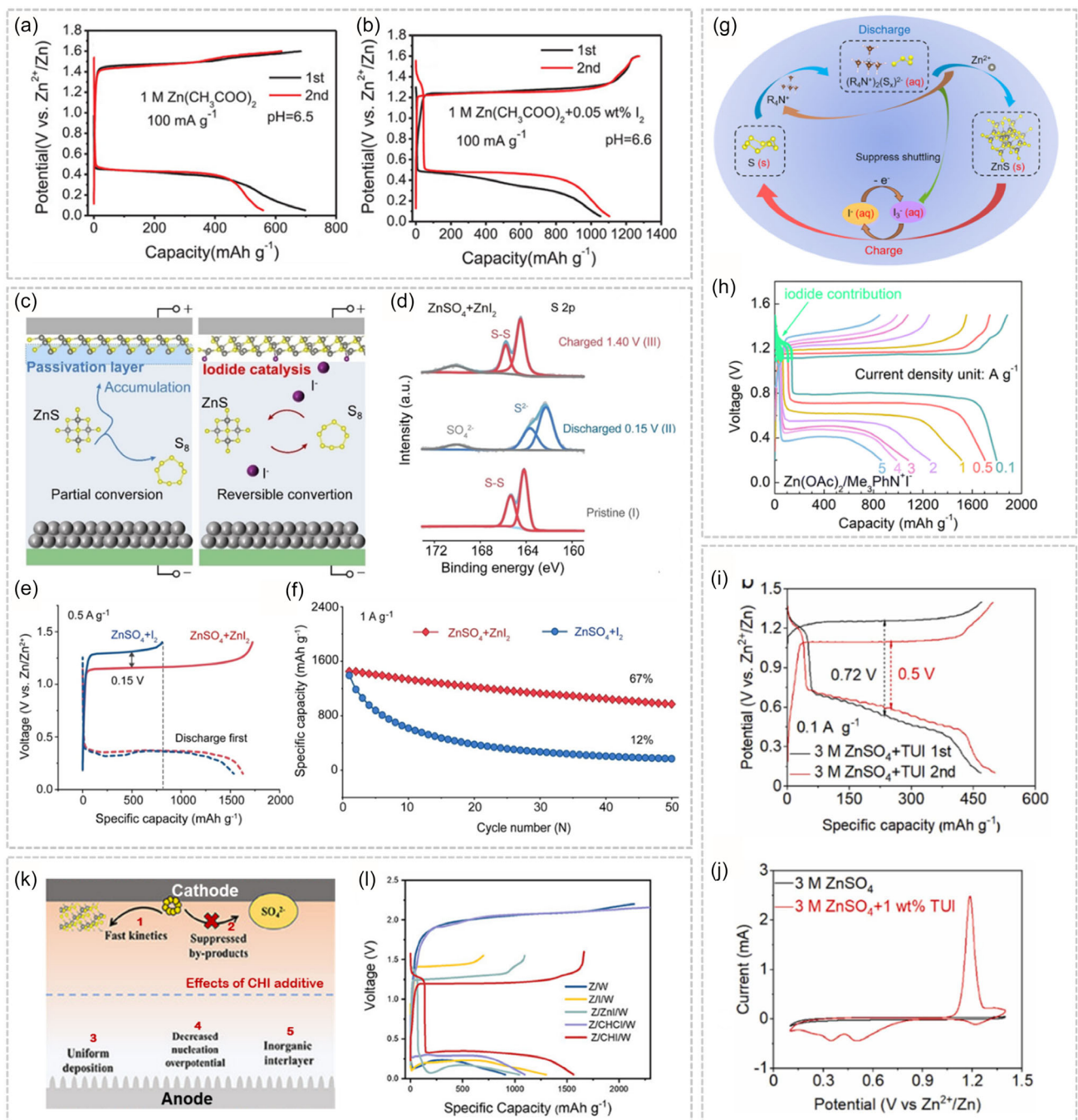


Figure 7. Iodide-based redox mediator. a) GCD profile of S-based cathode in 1 M $\text{Zn}(\text{CH}_3\text{COO})_2$, and b) 1 M $\text{Zn}(\text{CH}_3\text{COO})_2$ with I_2 as additive. This panel was reproduced with permission.^[21] Copyright 2020 Wiley. c) Schematic diagram of the I^- ion catalytic mechanism. d) S 2p XPS spectra recorded at various charge states using a $\text{ZnSO}_4 + \text{ZnI}_2$ electrolyte. e) Initial charge/discharge curves in different electrolytes. f) Comparing cyclic performance of the AZSB using ZnI_2 and I_2 additive. This panel was reproduced with permission.^[31] Copyright 2024 Wiley. g) Schematic illustrating sulfur redox pathway in AZSBs using R_4N^{+} -dual mediator system. h) Galvanostatic charge-discharge (GCD) performance with $\text{Zn}(\text{CH}_3\text{COO})_2/\text{Me}_3\text{PhN}^+\text{I}^-$ electrolyte at various current densities. This panel was reproduced with permission.^[30] Copyright 2023 Royal Society of Chemistry. i) Voltage profiles of cells incorporating the TUI additive. j) Cyclic Voltammetry of ZnS@CF in 3 M ZnSO_4 in the absence and presence of TUI additive. This panel was reproduced with permission.^[88] Copyright 2022 Elsevier. k) Representation of CHI role on the sulfur cathode and Zn anode. l) GCD profile for various electrolytes in AZSBs. This panel was reproduced with permission.^[85] Copyright 2025 Wiley.

redox mediator, enhanced the performance and durability of AZSB (Figure 7k).^[85] On the cathode side, CHI not only interacts with ZnS and accelerates ZnS oxidation by elongating the Zn–S bond but also forms a protective layer that suppresses the side

reactions involving H_2S , SO_4^{2-} , and water decomposition, thus improving its redox reversibility. On the anode side, CHI reduces nucleation overpotential, minimizes electric field distortions, and facilitates uniform Zn deposition through electrostatic shielding.

As a result, the AZSB achieves a high discharge capacity of 1666 mAh g^{-1} (1 A g^{-1}) and shows a significant reduction in nucleation overpotential from 31.9 mV in bare electrolyte to 11.5 mV in CHI modified electrolyte (Figure 7l).

4.3.2. Thiourea-Based

Thiourea (TU), a simple organosulfur compound, has emerged as a promising multifunctional additive for AZSBs.^[89] Owing to its unique chemical structure, featuring reactive C = S and N–H bonds, thiourea exhibits strong coordination abilities with Zn²⁺ ions and sulfur species. These properties allow thiourea to actively participate in electrochemical processes, modulate interfacial reactions, and stabilize electrode materials. Recent studies have demonstrated the dual functionality of thiourea in AZSBs, where it facilitates ZnS to S conversion kinetics in one approach and suppresses sulfur-water side reactions in another, highlighting its versatile role in enhancing battery performance.

Chang et al. proposed TU, a novel bifunctional electrolyte to enhance ZnS–S conversion kinetics and boost overall capacity.^[84] In their study, carbonium ions in the intermediate of TU preferentially interact with sulfur atoms in ZnS rather than with the hydrogen atom of water molecules, thereby suppressing the formation of SO₄²⁻ byproducts and promoting a more stable electrochemical process (Figure 8a). The conjugated system of TU facilitates electron redistribution under an external electric field during discharge, leading to the heterolytic cleavage of C = S bonds and the generation of C = N bonds. As the process continues, unstable TU further decomposes, generating HN = C=NH (Met) and S²⁻ ions, which then interact with Zn²⁺ to form zinc sulfide. During charging, this reaction reverses as negatively charged sulfur atoms of TU and nitrogen lone pairs interact with ZnS, lowering the bond energy and enabling easier dissociation into Zn²⁺. Additionally, the intermediate Met⁺ formed during charging enhances this effect by further weakening ZnS bonds as its positively charged center interacts with the S of zinc sulfide, lowering the bond energy between them and promoting faster conversion. Experimental measurement, particularly the galvanostatic intermittent titration technique (GITT) (Figure 8b), confirms the role of TU in increasing Zn²⁺ diffusion, reducing polarization, and improving overall kinetics.

Further, Li et al. leveraged the surface-active properties of thiourea to address sulfur-water disproportionation reactions, a major cause of capacity fading.^[50] They proposed a novel "raincoat" strategy, wherein DFT calculations suggest that thiourea as an organic ligand additive, preferentially adsorbs on the ZnS surface and forms an *in situ* metal–organic complex protecting layer on the S-cathode. Further, a narrow energy gap observed in Zn²⁺-TU ligand complex suggests improved electron transfer capability. Thus, this raincoat-like layer blocks the direct contact between sulfur and the aqueous electrolyte while enabling efficient Zn²⁺ transport (Figure 8c). The TU molecules strongly adsorb onto the ZnS cathode surface, preventing water-induced parasitic reactions and active material aggregation (Figure 8d). As a result, this approach delivers a high discharge capacity of 1478 mAh g^{-1} .

(0.1 A g^{-1}) and retains 53.3% of its capacity after 300 cycles at 2 A g^{-1} (Figure 8e). This strategy, proven effective for various sulfur-based cathodes, offers a universal solution to improve the cyclic stability and performance of AZSBs by effectively suppressing side reactions and improving cathode stability.

4.4. Hybrid/Organic Electrolytes

All of the aforementioned strategies have shown notable improvements in enhancing the kinetics of conversion reactions of sulfur and suppressing the side reaction at the sulfur cathode. However, challenges associated with the zinc anode, such as HER, zinc corrosion, and zinc dendrite formation, continue to hinder capacity retention and long-term performance. To simultaneously address these challenges on both the sulfur cathode and zinc anode side, hybrid electrolytes incorporating organic cosolvents or a combination of cosolvents and redox mediators in the aqueous electrolyte have proven as an effective solution due to their ease of formulation and demonstrated effectiveness.^[70] By adjusting the water-to-organic solvent ratio, researchers have aimed to optimize electrolyte properties while mitigating common issues of sulfur cathode as well as issues related to zinc anode. Specifically, organic cosolvents containing polar functional groups such as hydroxyl (-OH) in alcohols, carbonyl (-C=O) in ketones and aldehydes, amine (-NH₂), and ether (-O-) groups not only alter the solvation structure but also serve as electron donors, facilitating the evolution of I⁻ to I₃⁻.^[22,86] The resulting I₃⁻ polar catalysts significantly boost sulfur cathode conversion kinetics and ultimately enhance the electrochemical performance of the AZSB cells. These organic cosolvents not only help to regulate the solvation structure but also improve interfacial compatibility. Since organic solvent shows good wettability with the sulfur cathode, this approach favors faster Zn²⁺ ions transport kinetics, thereby reducing the voltage polarization and improving the overall efficiency of the AZSB. In this section, we will discuss various organic solvents that have been explored for formulating hybrid electrolytes, along with their respective impacts on the performance of AZSB full cells.

4.4.1. Polyethylene Glycol 400 (PEG-400)

AZSBs suffer from incomplete conversion due to uneven accumulation of ZnS on the cathode, due to uncontrolled aggregation of ZnS crystals, forming congested structures that hinder reversibility. Therefore, Zhou et al. proposed the ZnS nucleation-regulated strategy by introducing PEG-400 as an organic cosolvent into a 1 M Zn(CH₃COO)₂ electrolyte.^[29] Upon addition of PEG-400, it solvates Zn²⁺, and alters the solvation sheath that enables the formation of uniform and smaller ZnS discharge products (average size $\approx 180 \text{ nm}$), which promotes a more efficient and reversible ZnS to sulfur conversion with lower polarization (Figure 9a). As a result, the S@CNTs-50 cathode achieves a specific capacity of 1116 mAh g^{-1} with a low voltage hysteresis of 0.47 V (0.1 A g^{-1}) (Figure 9b), along with a high-rate capability of 774 mAh g^{-1} (1 A g^{-1}). The optimal H₂O-to-PEG-400 mass ratio (5:2) ensures

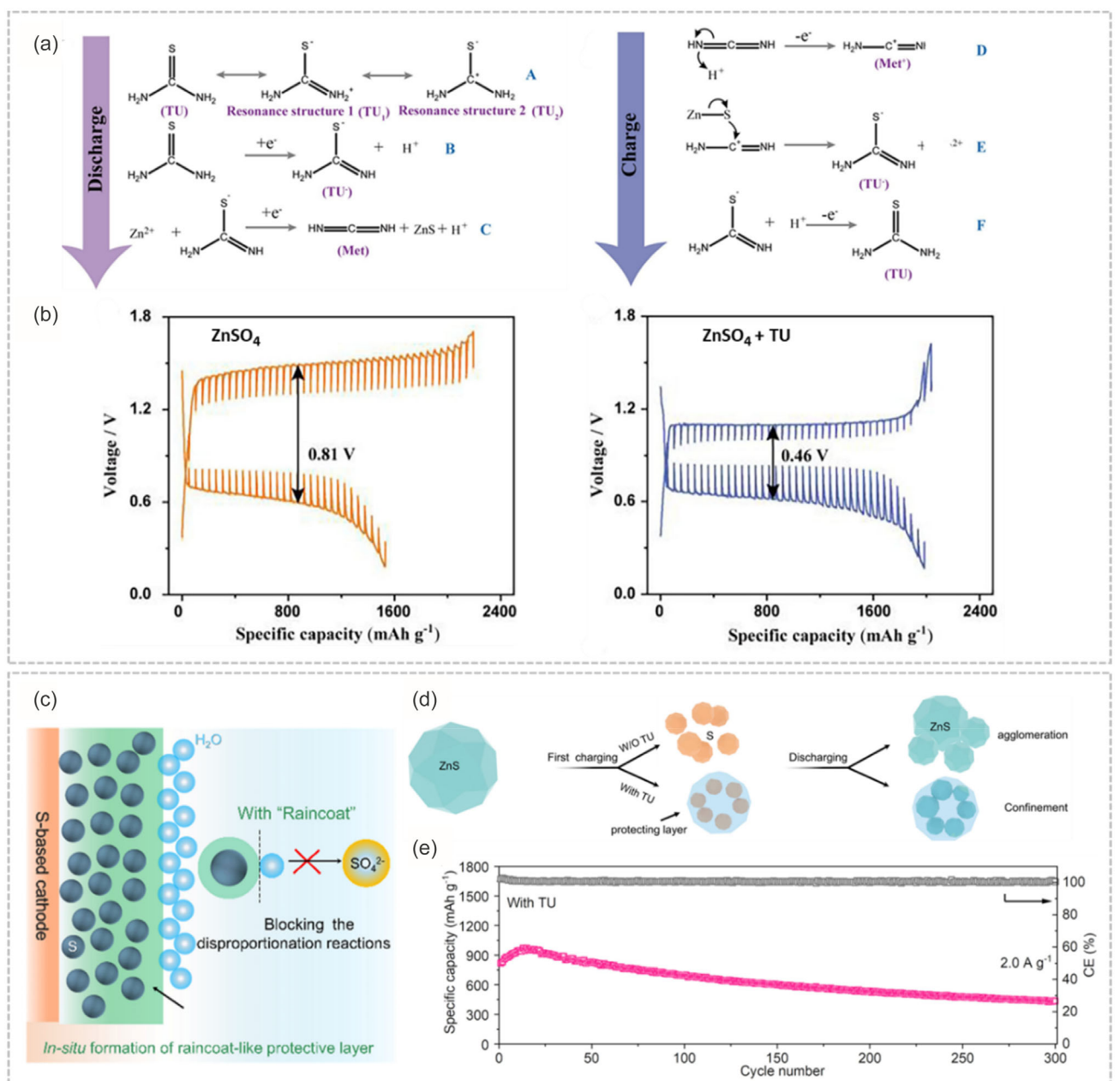


Figure 8. Thiourea-based redox mediator. a) The reaction pathway of TU during discharging and charging. b) GITT profiles of S@KB electrodes using ZnSO_4 electrolyte in the absence and presence of TU additive. This panel was reproduced with permission.^[84] Copyright 2023 Elsevier. c) Diagram showing the formation of a protective interfacial layer by adding TU as a ligand during charging. d) Schematic of the morphological evolution of ZnS cathode during the initial cycle, with and without TU. e) Long-term cycling test of AZSBs using TU-containing electrolytes. This panel was reproduced with permission.^[50] Copyright 2024 Elsevier.

the growth of ZnS into uniform spheres, facilitating stable charge-discharge cycles, while PEG also suppresses the dissolution of active materials. Notably, previous studies have reported the ability of PEG to stabilize Zn stripping and plating in AZIBs. Compared to conventional electrolytes, where $\text{Zn}||\text{Zn}$ symmetric cells suffer from early failure (lasting only 76 h in 1 M $\text{Zn}(\text{CH}_3\text{COO})_2$, however, PEG-based electrolyte significantly prolongs cycling stability to over 480 h (Figure 9c), despite slightly higher overpotentials due to increased viscosity.

4.4.2. Tetramethylene Sulfone (TMS)

Another nucleophilic regulation strategy was proposed by Shen et al. to modulate the oxidation kinetics of ZnS by adjusting the Zn-S bonding strength, where different organic nucleophilic groups are screened to identify the most effective candidate as a cosolvent.^[90] Theoretical calculations using DFT shown in Figure 9d, reveal that TMS exhibits the highest adsorption energy (E_{ads} : -1.27 eV) toward ZnS compared to other nucleophilic groups, such as carbonyl and hydroxyl, and even water molecules.

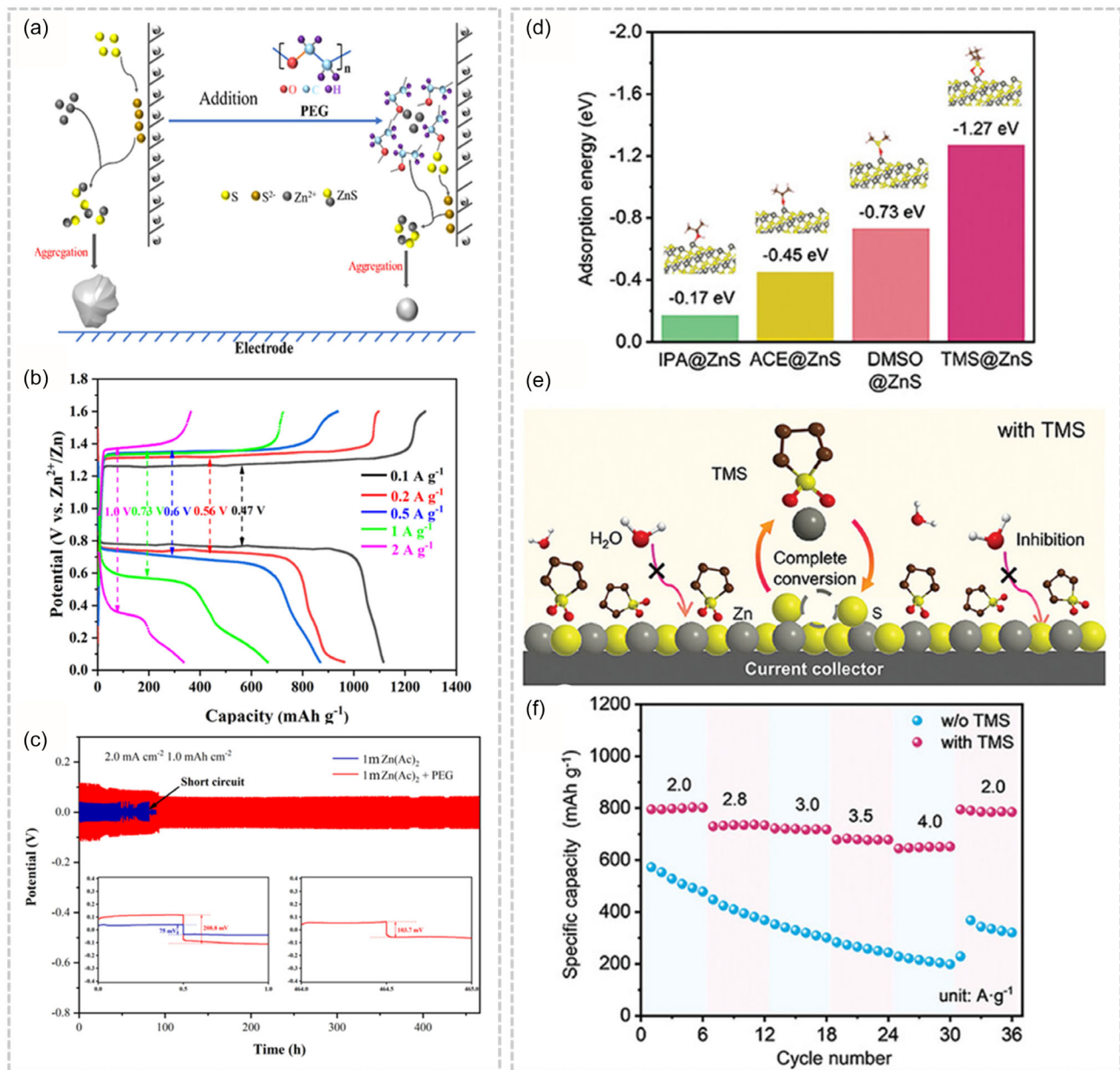


Figure 9. Organic cosolvents. a) The schematic representation of the effect of the introduction of PEG. b) GCD curves at various current densities. c) Galvanostatic cycling stability of Zn||Zn symmetric cells with or without PEG. This panel was reproduced with permission.^[29] Copyright 2022 Elsevier. d) Calculated adsorption energy (E_{ads}) of isopropanol (IPA), acetone (ACE), dimethyl sulfoxide (DMSO), and Tetramethylene sulfone (TMS) on ZnS. e) Illustration of the side-reaction inhibition mechanism by TMS. f) Rate performance test of cells in the presence and absence of TMS. This panel was reproduced with permission.^[90] Copyright 2024 Wiley.

(E_{ads} : -0.95 eV), indicating its superior ability to interact with ZnS and induce charge redistribution. Further, due to its strong interaction with Zn atoms in ZnS through its sulfone group, it lowers the oxidation energy barrier and facilitates the conversion of ZnS to sulfur (Figure 9e). This interaction not only accelerates the ZnS oxidation kinetics but also suppresses side reactions by shielding ZnS from active water molecules, thereby enhancing the utilization of active materials and ensuring a reversible solid-solid conversion. As a result, it shows good electrochemical performance, delivering a discharge capacity of 799 mAh g⁻¹ (2.0 A g⁻¹) and

649 mAh g⁻¹ (4.0 A g⁻¹), along with improved capacity retention after long cycles (Figure 9f).

4.4.3. Tetraglyme (G_4) and Iodine

Seeking the benefits of both cosolvent and redox mediator additives, Zhu et al. reported a “cocktail-optimized” aqueous electrolyte containing G_4 as cosolvent, I_2 as the redox mediator, and $Zn(CF_3SO_3)_2$ as salt, aiming to boost electrode reversibility and suppress side reactions (Figure 10a).^[26] Computational

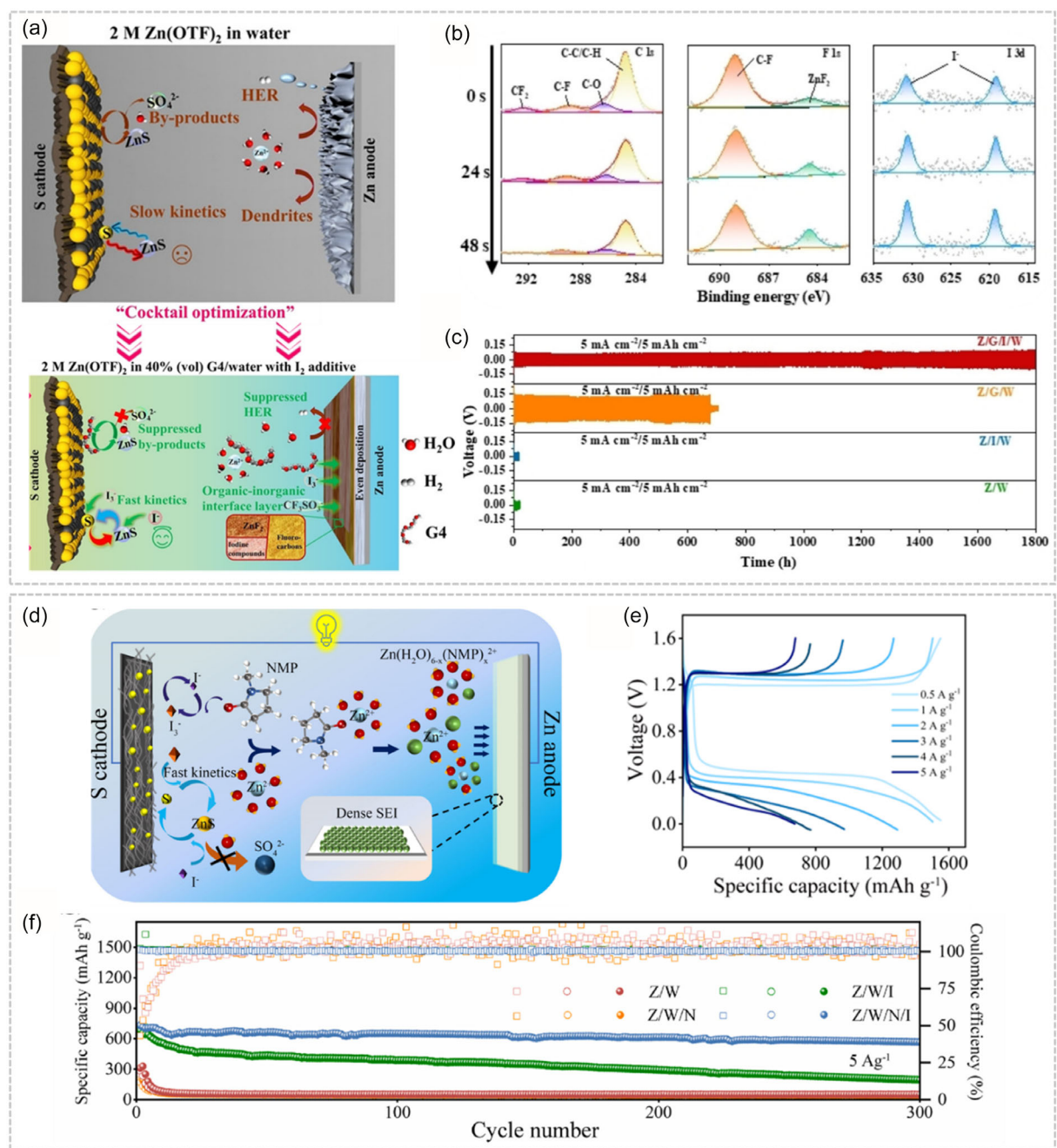


Figure 10. Hybrid electrolytes. a) Schematic comparison of AZSBs using two electrolyte systems: Z/W (up) and Z/G/I/W electrolyte (down). b) XPS analysis of the zinc anode after 15 cycles in Z/G/I/W electrolyte. c) Zn||Zn symmetric cell performance in the various electrolytes. This panel was reproduced with permission.^[26] Copyright 2022 Wiley. d) Schematic representation of the synergistic effect between KI and NMP. e) GCD profile using Z/W/I electrolyte at different current. f) Cyclic performance comparison between the NMP-optimized electrolyte with different electrolyte systems. This panel was reproduced with permission.^[86] Copyright 2024 Elsevier.

investigations showed that the glycol dimethyl ether (G₄) molecule exhibits a lower E_{ads} value than water on both S and ZnS surfaces, indicating its strong affinity for the S cathode in both charged and discharged states. This helps to improve electrolyte wettability and blocks water access, inhibiting the formation of SO₄²⁻ during sulfur conversion. Simultaneously, the I₂ additive is reduced to I₃⁻ polyanions by the electron-donating group ($-\text{COC}-$) of G₄, creating an efficient polar I₃⁻/I⁻ catalyst couple

that lowers polarization, reduces activation energy, and enhances the solid-solid conversion of sulfur. G₄ also stabilizes the zinc anode by forming an organic-inorganic hybrid solid electrolyte interphase (SEI) evidenced by XPS upon cycling (Figure 10b). The C 1s spectrum shows the presence of organic groups such as C-C/C-H, C-O, C-F, and CF₂, indicating the decomposition of the G₄-Zn(OTF)₂ complex and partial reduction of OTF⁻ anions. The F 1s spectrum shows the formation of inorganic ZnF₂, while

the I 3d spectrum suggests the presence of I^- species originating from I_2 . These findings confirm that the SEI consists of both organic and inorganic components, which shield the zinc anode surface from H_2O and guides Zn^{2+} ion diffusion, ensuring a long cycle life of up to 1800 h at 5 mA cm⁻² with 5 mAh cm⁻² in $\text{Zn}||\text{Zn}$ symmetric cells (Figure 10c).

4.4.4. N-Methylpyridine (NMP) and Potassium Iodide (KI)

To improve the positive electrode reversibility and negative electrode stability, another novel hybrid electrolyte is developed by incorporating NMP and KI (Figure 10d).^[86] The presence of an electrophilic group in NMP promotes the I^- oxidation to I_3^- , forming a redox mediator that accelerates sulfur conversion reactions, lowers energy barriers, and inhibits unwanted side products. Simultaneously, it also changes the solvation environment of $\text{Zn}(\text{H}_2\text{O})_6^{2+}$, replacing H_2O in the solvated shell, ensuring uniform Zn^{2+} deposition and suppressing dendrite formation. Stabilized zinc plating and stripping are further assisted by the formation of nitrogen-rich SEI layer at the Zn surface with the presence of pyrrolic C—N, pyridinic C—N, ZnCO_3 , C—N/C—O, and sp^3 C—C/C—H groups as confirmed by XPS. The synergistic effects of NMP and KI provide a specific capacity of 1549 mAh g⁻¹ (0.5 A g⁻¹) with capacity retention of 77.5% after 300 cycles at 5 A g⁻¹ (Figure 10e,f).

4.4.5. Ethylene Glycol (EG) and ZnI_2

Ethylene glycol (EG) is a promising cosolvent due to its antifreezing properties (freezing point -12.9°C), excellent water miscibility, high dielectric constant (37.5), and two -OH functional groups per molecule that form strong hydrogen bonds with water.^[49] MD studies confirm that the addition of EG modifies the solvation structure of Zn^{2+} ions and reduces free water activity, effectively suppressing water-related side reactions and reducing Zn electrode corrosion.^[22] Additionally, EG is believed to form a protective SEI layer on the Zn anode, further stabilizing the electrode-electrolyte interphase.^[49] Guo et al. proposed a facile approach using EG as a cosolvent and ZnI_2 as an additive in $\text{Zn}(\text{CF}_3\text{SO}_3)_2$ -based aqueous electrolyte and found that the stronger hydrogen bonding environment in their modified electrolyte not only enlarges the ESW of the electrolyte but also mitigates sulfur side reactions and Zn dendrites formation (Figure 11a).^[22] Interestingly, this study reveals a multistep conversion reaction pathway in the hybrid electrolyte, differing from the one-step conversion observed in pure aqueous systems. During discharge, elemental sulfur undergoes sequential reduction from long-chain to short-chain zinc polysulfides and ultimately to ZnS ($\text{S}_8 \rightarrow \text{S}_x^{2-} \rightarrow \text{S}_2^{2-} + \text{S}^{2-}$). During charging, zinc sulfide and short-chain polysulfides undergo oxidation to regenerate elemental sulfur, which was supported by Raman (Figure 11b). During discharge (state-b to state-d), three distinct peaks appear at 317, 420, and 610 cm⁻¹, corresponding to polysulfides (S_x^{2-}), disulfides (S_2^{2-}), and sulfides (S^{2-}), respectively. The S_2^{2-} peak becomes stronger upon discharging, and some of it further converts to S^{2-} at the full discharge. Upon recharging (state-d to state-g),

the S_x^{2-} peak reappears, while the S^{2-} and S_2^{2-} peaks start to disappear, indicating a reversible reaction back to higher-order sulfur species. Eventually, all polysulfide-related peaks vanish and elemental sulfur peaks regenerate at full charge, confirming the reversibility of the S to ZnS conversion. These findings are further confirmed by XPS analysis, which shows the presence of terminal sulfur (S_T^{-1}) and sulfide (S^{2-}) species during discharge (Figure 11c). The persistence (presence) of S_T^{-1} at full discharge suggests the presence of ZnS and ZnS_2 , likely due to sluggish reaction kinetics. Upon charging, the S_T^{-1} and S^{2-} peaks gradually disappear, and the peak of bridging sulfur (S_B^0) is observed, indicating the oxidation of ZnS and ZnS_2 back to elemental sulfur. This spectroscopic investigation thus confirms a multistep reversible chemical conversion mechanism facilitated by the hybrid electrolyte system and provides advanced insights into the AZSB with opening new pathways for designing high-performance batteries.

4.4.6. Dimethyl carbonate (DMC) and Iodine

DMC is a nonpolar, aprotic solvent widely known for its low toxicity and excellent biodegradability. To tackle water-based side reactions and improve cathode wettability in AZSBs, Patel et al. utilize 40% DMC and I_2 to develop a hybrid electrolyte.^[91] The developed AZSBs cells with hybrid electrolyte and biowaste-derived carbon achieve a specific capacity of 1167 mAh g⁻¹ (0.1 A g⁻¹) with retention of 47.6% capacity after 200 cycles at 1 A g⁻¹, showing excellent cycling stability (Figure 12a,b). This approach offers a promising, eco-friendly solution for high-performance AZSBs with an energy density of 502 Wh kg⁻¹.

4.4.7. Dimethylacetamide (DMA) and ZnI_2

In the series of hybrid electrolytes, Thomas et al. investigated DMA as a high-donor-number organic cosolvent and ZnI_2 as an additive in $\text{Zn}(\text{CF}_3\text{SO}_3)_2$ solution to enhance AZSB performance (Figure 12c).^[92] Via different characterizations, it is found that the novel electrolyte suppresses parasitic reactions, reconstructs the solvation structure of Zn^{2+} by replacing H_2O molecules, and enhances reversibility of electrode reactions. With these interventions, the electrolyte allows the cells to deliver a high specific capacity of 1453 mAh g⁻¹ (0.1 A g⁻¹) (Figure 12d) and retain 72% of the capacity after 300 cycles at 5 A g⁻¹.

4.4.8. Acetonitrile (AN) and Iodine

In the series of hybrid electrolytes for AZSBs, Ge et al. explored usage of acetonitrile and modified $\text{Zn}(\text{CF}_3\text{SO}_3)_2$ -based aqueous electrolyte with varying volume ratios of water and acetonitrile.^[93] Trace amounts of iodine (I_2) were dissolved for the purpose of redox mediation at the cathode. At the anode, the hybrid electrolyte effectively suppressed HER at negative potentials, promoted uniform Zn^{2+} stripping/plating, and mitigated parasitic reactions and zinc corrosion. Improving the interaction between the sulfur cathode and the electrolyte, and accelerating the

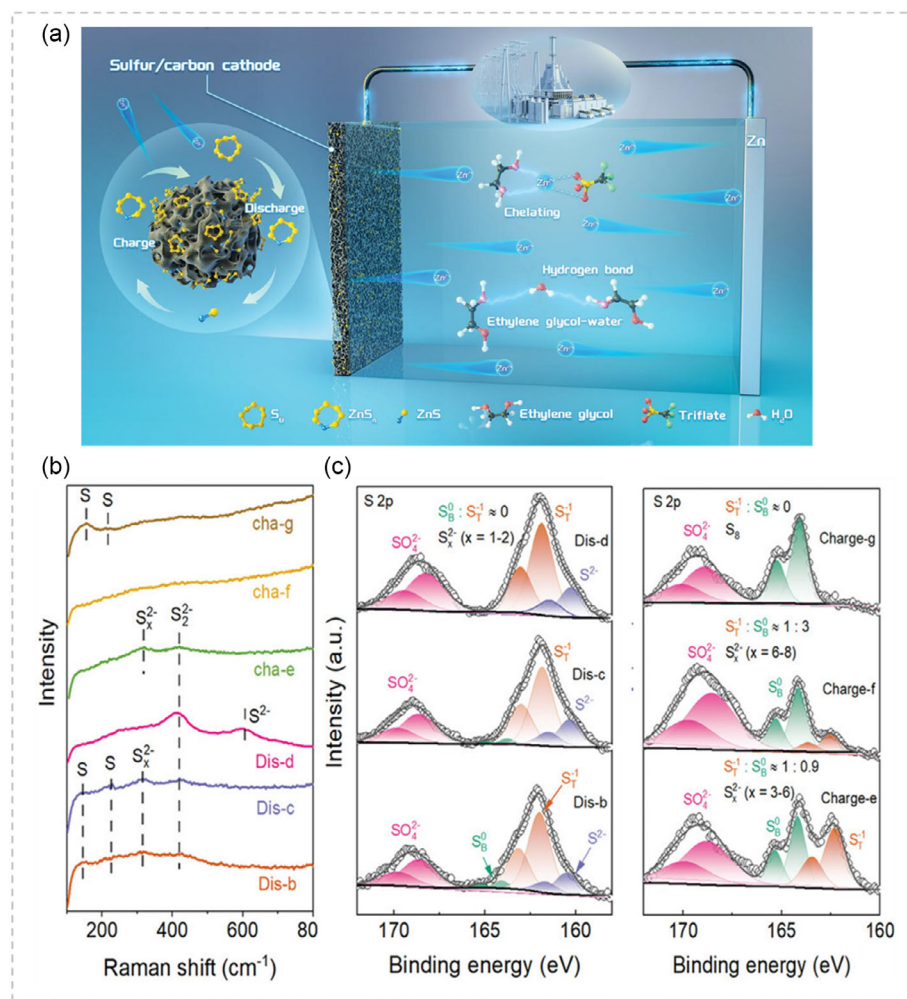


Figure 11. Hybrid electrolytes. a) Representation of an AZSB system using EG-based hybrid electrolyte. b) Raman spectra and c) XPS spectra of 50-S@NPC at various charge–discharge states showing multistep pathway. This panel was reproduced with permission.^[22] Copyright 2023 Wiley.

diffusion of Zn^{2+} ions, also reduced charge transfer resistance (R_{ct}) (Figure 12e) in the cell. Among the tested different combinations, the electrolyte with a 1:1 water/AN ratio (Figure 12f) delivered an excellent specific capacity of 1370 mAh g^{-1} with a CE of 79.9%, along with high-rate capability and cycling stability.

4.4.9. Propylene Glycol Methyl ether (PM) and ZnI_2

Another novel electrolyte engineering strategy for AZSB was proposed by introducing PM as a cosolvent in combination with a ZnI_2 additive (Figure 12g).^[48] This innovation effectively restructures the electrolyte network to address two major challenges—sluggish sulfur redox kinetics and zinc dendrite formation. The lone pair of electrons on the oxygen atom in PM attracts the Zn^{2+} to form PM- Zn^{2+} coordination, contributing to the modified electrolyte structure. To investigate this, RDF and CN analysis were performed using MD simulations, indicating the presence of OTF^- and PM in the Zn^{2+} solvation shell due to their strong coordination ability. Moreover, the PM cosolvent, with its polar functional groups (-OH and C—O—C), not only enhances the

redox activity of the I^-/I_3^- mediator—reducing the energy barrier and accelerating sulfur conversion reactions (Figure 12h,i)—but also modifies the Zn/electrolyte interface to promote uniform Zn plating. This dual-functional approach significantly improves interfacial stability and reaction reversibility, resulting in high discharge capacity and excellent cycling performance. The study highlights a powerful cosolvent design principle that enables simultaneous optimization of both cathodic and anodic processes in AZSBs.

Through deliberate tailoring of electrolyte structure, researchers have achieved enhanced reversibility at the electrodes, suppression of parasitic reactions, and extended battery life. The above-discussed advancements in hybrid electrolytes underscore the synergistic role of cosolvents and redox mediators in simultaneously enhancing cathode kinetics and stabilizing the anode interface in Zn–S batteries. The growing diversity of hybrid electrolyte design strategies offers valuable insights into developing next-generation energy storage systems with enhanced efficiency and stability. A concise comparative overview of these strategies is presented in Table 1.

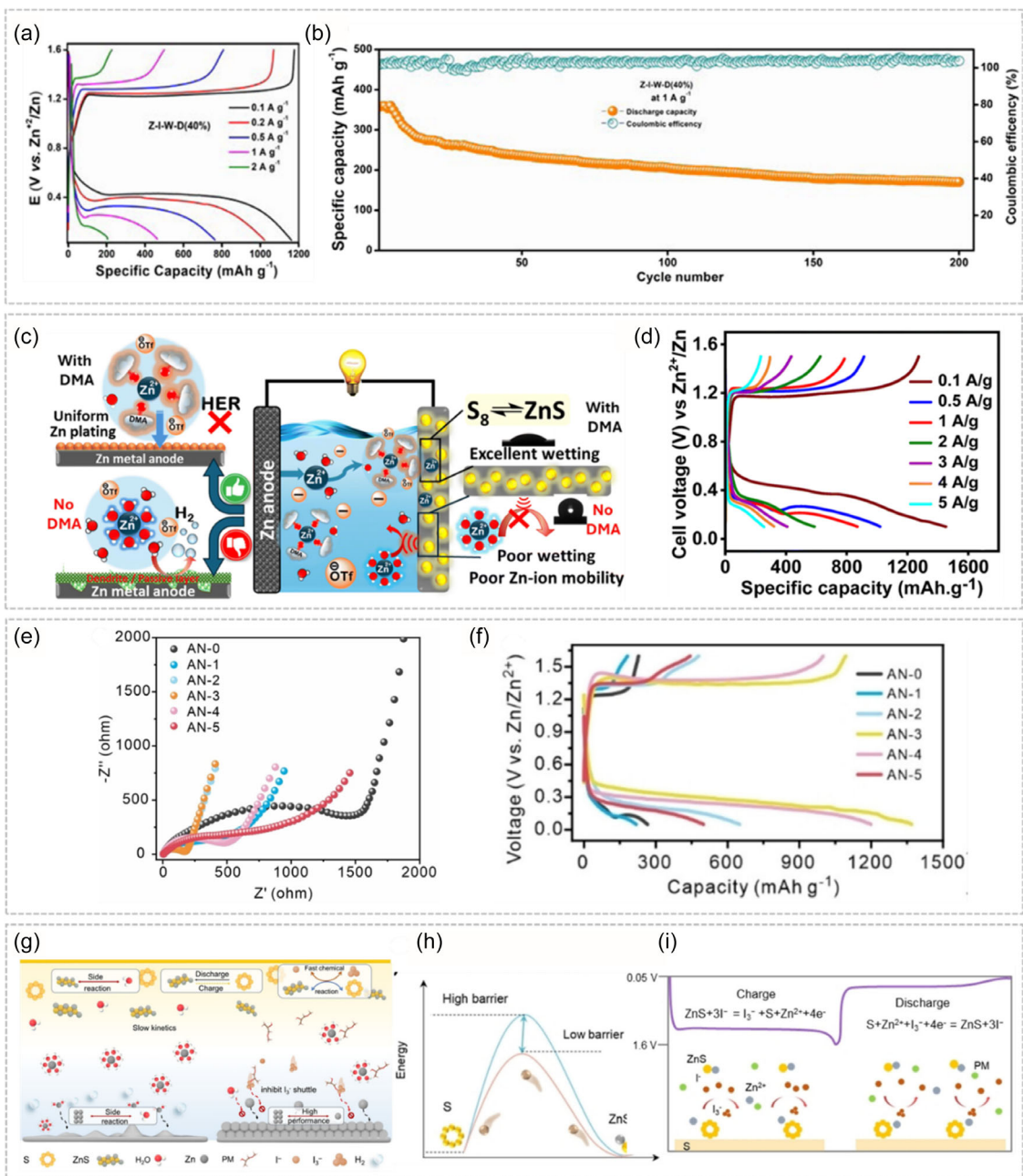


Figure 12. Hybrid electrolytes. a) GCD profile curves in Z-I-W-D electrolyte at different current densities. b) Cycling performance for AZSB in Z-I-W-D electrolyte at current density 1 A g^{-1} . This panel was reproduced with permission.^[91] Copyright 2024 Elsevier. c) Schematic illustration of the effect with or without DMA as a cosolvent in aqueous electrolyte of AZSB. d) Charge-discharge curves using AZ/D/ZnI₂ electrolyte at various current densities. This panel was reproduced with permission.^[92] Copyright 2024 Royal Society of Chemistry. e) Nyquist plots of fresh AN-X based AZSBs indicating the presence of charge transfer resistance (R_{ct}), with noticeable differences in semicircle diameters. f) Discharge/charge curves of AN-X based AZSBs at the 1st cycle. This panel was reproduced with permission.^[93] Copyright 2024 Wiley. g) Illustrative diagram of AZSB in different electrolyte systems (left) with 1 M Zn(CF₃SO₃)₂ in H₂O electrolyte and (right) with 1 M Zn(CF₃SO₃)₂ in a PM/water mixture with zinc iodide (ZnI₂) additive. h) Conversion energy barriers for S and ZnS with or without PM. i) Schematic diagrams of the discharge and charge processes involving the iodine source and PM. This panel was reproduced with permission.^[48] Copyright 2024 Wiley.

4.5. Deep Eutectic Electrolytes

Deep eutectic solvents (DESs) have developed as a promising class of environmentally benign and sustainable solvents, gaining attention for their potential in green electrochemical systems.^[94]

Although DESs are not inherently aqueous, their relevance in zinc–sulfur batteries is growing due to their modular composition, which allows precise tuning of physicochemical properties and Zn²⁺ coordination behavior to meet specific electrochemical requirements. Furthermore, DESs are easy to synthesize, low-cost,

Table 1. Performance of various cosolvents and additives in various zinc salt-based electrolytes.

Sr. no.	Electrolyte	Co-solvents/ additives	Key role & effects	Initial discharge capacity [mAh g ⁻¹] / current density [A g ⁻¹]	Capacity retention/ cycle no./ current density [A g ⁻¹]	CE	Average voltage hysteresis during first cycle	Temperature resilience (−20 to 60 °C)	Cost impact compared to AZSB with bare aqueous electrolyte ^{b)}	Reference
1	Zn(CH ₃ COO) ₂	I ₂	Nonpolar redox mediator improves sulfur conversion kinetics.	1105/0.1	85%/50/1	≈100%	0.72	No	High—I ₂ is expensive despite Zn salt being cheap.	[21]
2	ZnSO ₄	ZnI ₂	Polar redox mediator generates abundant I [−] , improves sulfur conversion kinetics.	1744/0.5	100%/550/5	≈100%	0.8 ^{a)}	No	High—ZnI ₂ is costly and limits scalability.	[31]
3	Zn(CH ₃ COO) ₂	Me ₃ PhN ⁺ I [−]	Dual-functional redox mediator improves sulfur conversion kinetics, generates soluble polysulfides.	1659/0.1	89%/50/3	≈100%	0.34	No	Moderate—additive is expensive.	[30]
4	ZnSO ₄	TU ^{c)}	Redox mediator: reduces the activation barrier of ZnS conversion.	1410/0.1	65%/300/2	≈100%	0.5	No	Moderate—TU is cheap, but synthesis of TU adds cost.	[88]
5	Zn(CF ₃ SO ₃) ₂	CHI	Dual-functional redox mediator improves sulfur conversion kinetics, inhibits sulfur side reaction, dendrite-free Zn.	1666/1	58.8%/30/1	≈95.4%	0.82 ^{a)}	No	High—Triflate salt is expensive.	[85]
6	ZnSO ₄	TU	Bifunctional redox mediator improves sulfur conversion kinetics, inhibits sulfur side reaction.	1740/0.5	51%/300/5	≈100%	0.46	No	Low—Both TU and ZnSO ₄ are highly cost-effective.	[84]
7	ZnSO ₄	TU + ZnI ₂	Organic ligand additive: formation of cathode electrolyte interphase (CEI), inhibits sulfur side reaction, improves sulfur conversion kinetics.	1478/0.1	53.3%/300/2	≈100%	0.5 ^{a)}	No	High—ZnI ₂ dominates the cost.	[50]
8	Zn(CH ₃ COO) ₂	PEG-400	Modify the solvation sheath of Zn ²⁺ , uniform ZnS nucleation on cathode with a 180 nm size.	1116/0.1	81%/300/1	≈100%	0.47	No	Low—PEG is affordable and scalable.	[29]
9	ZnSO ₄	TMS	Nucleophilic regulation strategy, boosts Zn-S oxidation kinetics.	799/2	81.7%/200/2.8	≈100%	0.9 ^{a)}	No	Low—Additive cost is reasonable.	[90]
10	Zn(CF ₃ SO ₃) ₂	G4 + I ₂	Stabilize Zn anode, forming organic-inorganic SEI; facilitate conversion kinetics and suppress interfacial side reactions.	1140/0.5	70%/50/4	≈100%	0.8 ^{a)}	No	High—Triflate + I ₂ significantly increase cost.	[26]
11	Zn(CF ₃ SO ₃) ₂	NMP + KI	Improves sulfur conversion kinetics, anode stability by formation of SEI layer.	1491/1	77.5%/300/5	≈100%	1.0	No	High—NMP is costly; KI is moderate.	[86]
12	Zn(CF ₃ SO ₃) ₂	EG + ZnI ₂	Facilitate a multistep conversion reaction, eliminate sulfur side reactions, inhibit Zn dendritic growth.	1435/0.1	70%/250/3	≈100%	0.88	Yes	High—ZnI ₂ is cost-prohibitive.	[22]
13	Zn(CF ₃ SO ₃) ₂	DMC + I ₂	Improves sulfur conversion kinetics, enhances wettability of the sulfur cathode, stabilizes the Zn anode.	1167/0.1	47.6%/200/1	≈100%	0.8 ^{a)}	No	High—I ₂ and organic solvents raise cost.	[91]

Table 1. Continued.

Sr. no.	Electrolyte	Co-solvents/ additives	Key role & effects	Initial discharge capacity [mAh g ⁻¹] / current density [A g ⁻¹]	Capacity retention/ cycle no./ current density [A g ⁻¹]	CE	Average voltage hysteresis during first cycle	Temperature resilience (-20 to 60 °C)	Cost impact compared to AZSB with bare aqueous electrolyte ^{b)}	Reference
14	Zn(CF ₃ SO ₃) ₂	DMA + ZnI ₂	Improves sulfur conversion kinetics, suppresses HER and Zn corrosion.	1453/0.1	72%/300/5	≈95%	0.8 ^{a)}	No	High—Both DMA and ZnI ₂ are costly.	[92]
15	Zn(CF ₃ SO ₃) ₂	AN + I ₂	Improves sulfur conversion kinetics, suppresses HER and Zn corrosion.	1370/0.1	66.7%/25/0.1	≈79.9%	1 ^{a)}	No	High—AN and I ₂ increase overall cost.	[93]
16	Zn(CF ₃ SO ₃) ₂	PM + ZnI ₂	Improves sulfur conversion kinetics, improves interfacial stability of Zn anode.	1456/0.2	70%/1200/3	≈100%	0.99	No	High—PM and ZnI ₂ are both costly.	[48]

^{a)}Values calculated from the given graph; ^{b)}Conclusions drawn from chemical prices retrieved from <https://www.sigmaaldrich.com>.

and biodegradable, and they offer the additional advantage of excellent electrochemical and thermal stability.^[95] These solvents are formed by combining hydrogen bond donors (HBDs) with hydrogen bond acceptors (HBAs).^[96,97] However, their inherent high viscosity and low ionic conductivity pose limitations for ion transport. To overcome this, the addition of a controlled amount of water or aqueous solvent has proven effective in improving ionic mobility while maintaining the favorable properties of DESs.^[98–100] Although water-based eutectic electrolytes have not yet been explored for AZSBs, this hybrid approach can hold great promise for advancing their performance and stability of AZSBs. Therefore, this section highlights recent advancements in the field of DES-based systems tailored for Zn-S energy storage systems.

First, Cui et al. developed a cost-effective DES comprising choline chloride and urea (2:1) to enhance the electrochemical stability of Zn-S batteries (ZSBs) (Figure 13a).^[101] This DES exhibited excellent solubility for different Zn salts (e.g., ZnCl₂, ZnSO₄, Zn(NO₃)₂, Zn(CH₃COO)₂) with adequate ionic conductivity, and a wide ESW, effectively suppressing parasitic reactions and mitigating Zn dendrite formation. The optimized DES electrolyte effectively ensures dendrite-free zinc stripping/plating over 3920 h, significantly improving Zn anode cycling stability (Figure 13b). Experimental characterizations confirmed the formation of a stable SEI layer consisting of Zn, N, C, O, and Cl, facilitating homogeneous and rapid Zn²⁺ transport. Consequently, the ZSB demonstrated a high discharge capacity of 846 mAh g⁻¹

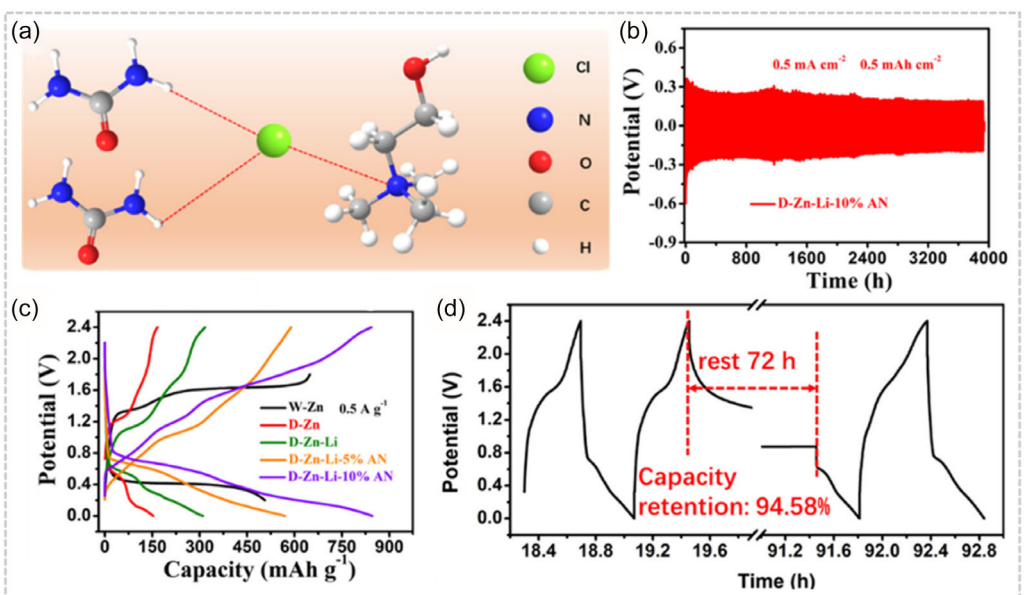


Figure 13. Deep eutectic electrolytes. a) Schematic representation of the ChCl/urea DES. b) Cycling performance of Zn/Zn symmetrical cells in D-Zn-Li-10% AN electrolyte. c) GCD profile in various electrolytes. d) GCD curves before and after a 72 h rest period at the full-charge state. This panel was reproduced with permission.^[101] Copyright 2021 American Chemical Society.

(0.5 A g^{-1}) with minimal self-discharge (94.58% capacity retention after 72 h) (Figure 13c,d).

The integration of DES into ZSBs can also address the long-standing electrochemical challenges associated with the sulfur cathode as demonstrated by Chen et al.^[102] Although sulfur boasts a high theoretical capacity, its low electrochemical reduction potential (S^0 to S^{2-}) inherently limits the discharge voltage (Figure 14a) while the formation of inert ZnS impedes the redox reversibility. To raise the output voltage, one might apply an overpotential to access higher oxidation states of sulfur. However, the widely used anions in aqueous systems (Figure 14b), such as OTF^- , SO_4^{2-} , AcO^- , and TFSI^- , are weak reductants and nucleophiles, unable to stabilize the positively charged sulfur species. As a result, these species tend to dissolve or decompose in aqueous solutions, leading to loss of active material and poor cyclic stability. Therefore, a stable electrolyte containing strongly nucleophilic anions is required to support efficient sulfur oxidation and reversible ZSBs. Chen et al. were the first to demonstrate a reversible S^{2-}/S^{4+} redox couple involving up to six-electron transfer in Zn-S batteries using a highly concentrated ClO_4^- -containing electrolyte.^[102] They employed a succinonitrile-Zn(ClO_4)₂ eutectic electrolyte, which stabilized positive sulfur species and minimized polarization. This breakthrough enabled a specific capacity of approximately 1284 mAh g⁻¹ and the highest reported operating voltage (1.54 V) in ZSBs, along with well-defined flat discharge plateaus. The battery exhibited robust sulfur conversion kinetics and cycling stability, retaining 85.7% capacity after 500 cycles (Figure 14c), and achieving an energy density of 527 Wh kg⁻¹. XPS and Raman spectroscopy (Figure 14d) confirmed multivalence sulfur conversion, with new S^{4+} ($\text{S}(\text{ClO}_4)_3^{+}$) peaks appearing during charging. DFT study further confirmed the six-electron transfer process, predicting a redox potential of S^{4+}/S^0 of 1.59 V (vs. Zn^{2+}/Zn) and highlighting the decisive role of ClO_4^- in stabilizing positively charged sulfur species. The cathode reaction involves two steps: 1) $\text{ZnS} \leftrightarrow \text{S} + \text{Zn}^{2+} + 2\text{e}^-$ and 2) $\text{S} + 3\text{ClO}_4^- \leftrightarrow \text{S}(\text{ClO}_4)_3^{+} + 4\text{e}^-$, coupled with $\text{Zn}^{2+} + 2\text{e}^- \leftrightarrow \text{Zn}$ at the anode (Figure 14e). The elevated discharge voltage indicates enhanced multivalent sulfur conversion enabled by the novel electrolyte. The succinonitrile-Zn(ClO_4)₂ design thus offers a powerful path to high energy, reversible sulfur batteries using a metal anode.

4.6. Solid-State/Hydrogel Electrolytes

With the increasing demand for smart and flexible electronic devices, solid-state and hydrogel-based electrolytes have shown great potential in the field of batteries. Solid-state/hydrogel electrolytes for aqueous batteries are often composed of water-soluble polymers such as polyvinyl alcohol, polyacrylic acid, and polyacrylamide. Replacing both the separator and aqueous solution in AZSBs, these electrolytes offer multiple advantages over aqueous systems, particularly in offering a leakage-proof matrix with high flexibility and mechanical integrity.^[27,67] Their enhanced mechanical strength helps suppress zinc dendrite growth, while their low water content reduces side reactions, thereby extending battery lifespan.^[103] The inherent flexibility

of these systems makes them compatible for easy integration into wearable and structurally adaptive devices.

Zhang et al. were among the first to report a quasi solid-state Zn-S battery, utilizing a ZnSO_4 -based PVA polymer electrolyte to realize a flexible, leak-proof device without capacity degradation under various deformation states.^[67] The fabricated solid-state cell, employing the $\text{Fe}(\text{CN})_6^{4-}$ doped composite cathode, achieved an energy density of 375 Wh kg^{-1} of sulfur and retained 56% of its capacity over 50 cycles at a very low current. Further developments in the field have focused on tailoring the solid-state or hydrogel-based electrolyte properties with the addition of copolymers, crosslinking agents, and functional additives. This search was also guided by the need to enhance the electrochemical performance of AZSB under extreme environmental conditions, such as hot or cold weather. In this regard, Amiri et al. developed a multifunctional quasisolid-state AZSB employing a freeze-resistant hydrogel electrolyte composed of $\text{Zn}(\text{CH}_3\text{COO})_2$, EG as an antifreezing agent, and iodine as a redox mediator additive.^[104] This formulation enabled wide-temperature operation (-25°C to $+25^\circ\text{C}$) and improved the redox kinetics by reducing the reaction barrier. Thus, the assembled quasisolid-state Zn-S battery delivers a high energy density of 283 Wh kg^{-1} . Expanding on their previous work, the same group further advanced the concept by developing a kirigami-inspired quasisolid-state Zn-S battery incorporating an antifreezing hydrogel electrolyte with improved mechanical adhesiveness.^[27] Retaining EG and iodine as the antifreezing agent and redox mediator, respectively, they systematically investigated the influence of different zinc salts, including $\text{Zn}(\text{CH}_3\text{COO})_2$, (ZnAc) , $\text{Zn}(\text{BF}_4)_2$, (ZnBF) , $\text{Zn}(\text{CF}_3\text{SO}_3)_2$, and ZnSO_4 , on both electrochemical performance and adhesive strength. Through tensile adhesion tests, the adhesion strength was found as $\text{Zn}(\text{CF}_3\text{SO}_3)_2 > \text{ZnBF} > \text{ZnAc-ZnBF}$ (1:1 molar ratio) $> \text{ZnAc} > \text{ZnSO}_4$. While the ZnAc-EG/I_2 hydrogel displayed good electrochemical behavior, it suffered from poor adhesion and delaminated during bending and stretching. On the other hand, ZnBF - and $\text{Zn}(\text{CF}_3\text{SO}_3)_2$ -based electrolytes exhibited strong adhesion but inferior electrochemical performance. To overcome this trade-off, a hybrid electrolyte composed of ZnAc and ZnBF in a 1:1 molar ratio was formulated, achieving a favorable balance between performance and mechanical robustness, with high energy density and a notable adhesion strength of 33.5 kPa.

Another innovative design of I_2 added amphiphilic gel electrolyte for AZSBs was introduced by Pumera et al. which was found to develop good interfaces with electrodes and restrict the shuttle of iodide species.^[105] The cells fabricated with this electrolyte and $\text{Ti}_3\text{C}_2\text{T}_x$ decorated sulfur cathode offered good cycling and mechanical stability. The cells, even after multiple bending cycles at 90 and 180° , retained their capacity and electrochemical performance. Further extending the promise of flexible Zn-S batteries, a recent study demonstrated the practical viability of advanced S/NC-CoO cathodes using a polyvinyl alcohol (PVA)-based gel electrolyte with a high zinc-ion conductivity of $9.6 \times 10^{-3} \text{ S cm}^{-1}$.^[106] These cells with quasi solid electrolyte offered good electrochemical performance along with excellent electrochemical stability and

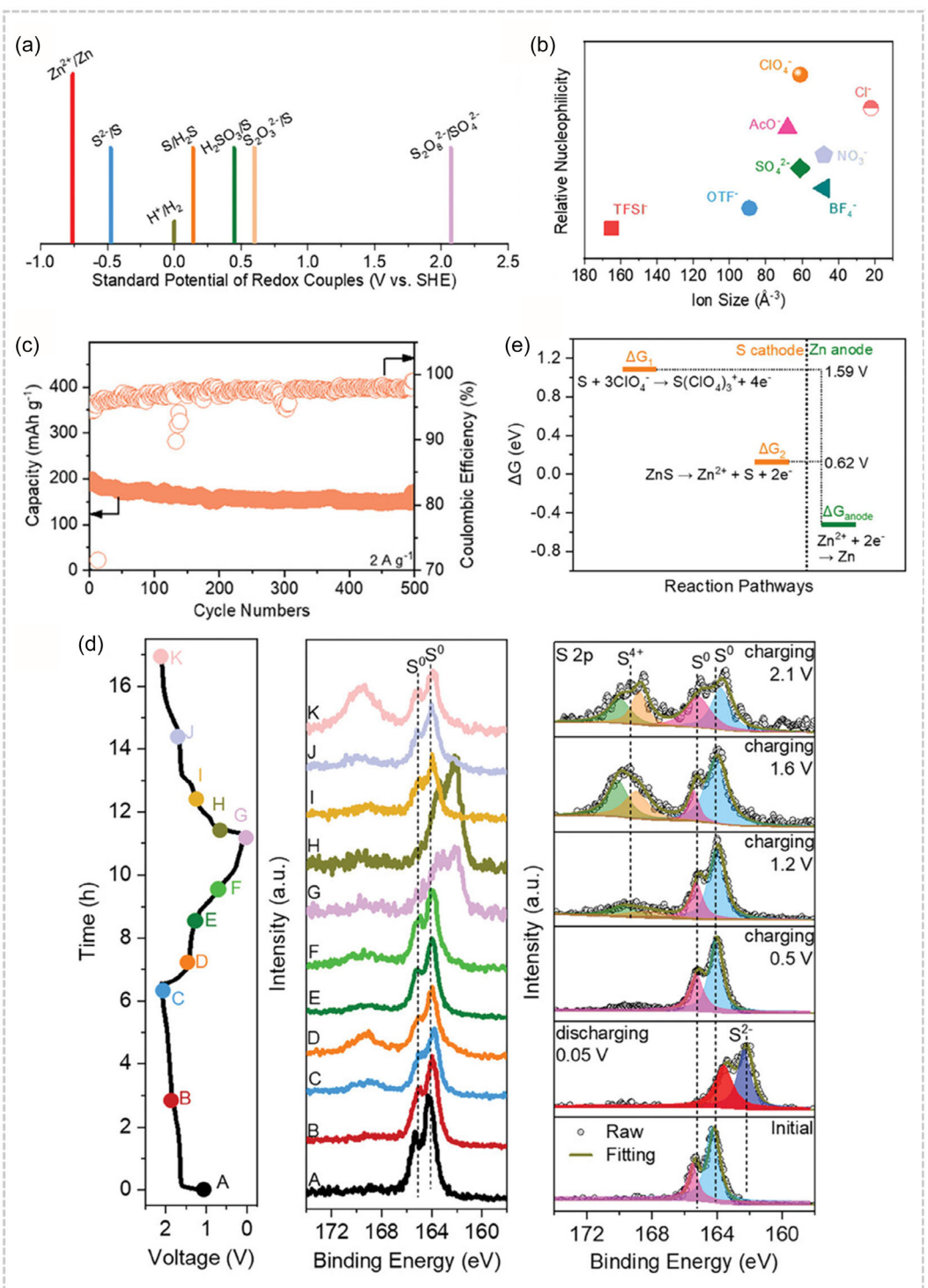


Figure 14. Deep eutectic electrolytes. a) Standard potentials of sulfur-based redox couples. b) Comparison of anion size and nucleophilicity. c) Cycling performance of the developed ZSBs. d) Investigation of the sulfur conversion mechanism using GCD curves and the corresponding XPS spectra and XPS fitting for S valence analysis. e) Theoretical calculations illustrating possible reaction pathways involved in the sulfur redox process. This panel was reproduced with permission.^[102] Copyright 2024 Wiley.

mechanical robustness. The assembled solid-state Zn-S cell delivered a good reversible capacity of 898 mAh g⁻¹ and a high energy density of 585 Wh kg⁻¹ of sulfur. The pouch cell operated stably for over 200 cycles with an average CE of

98.1%, and successfully powered a red LED at 1.8 V, which validates its practical potential for a wearable device. Collectively, the above studies highlight the growing potential of solid-state/hydrogel systems in enabling high-performance

AZSBs suitable for next-generation flexible energy storage applications.

5. Summary and Outlook

AZSBs stand out as a promising candidate for next-generation energy storage systems, owing to their high safety, low cost, and eco-friendly nature. However, it still encounters significant challenges, such as poor sulfur redox kinetics and loss of active material as SO_4^{2-} at the sulfur cathode, along with zinc corrosion and dendrite growth at the zinc anode. Overall, these problems hinder the practical application of AZSBs and limit their competitiveness with commercially established batteries.

The electrolyte plays a critical role in addressing the challenges associated with both the positive and negative electrodes in AZSBs. Therefore, this review focuses on recent advancements in electrolyte engineering for AZSBs, aiming to give a detailed understanding of the reaction mechanism and existing bottlenecks. This review presents an in-depth discussion of the problems faced by both the zinc anode and sulfur cathode in relation to electrolyte, along with the corresponding strategies proposed in recent years to optimize battery performance through electrolyte engineering. These strategies include tuning the electrolyte salt anion species, varying the electrolyte pH, and concentration of Zn-based salts, introducing redox mediators, additive engineering, incorporating cosolvents, and developing hybrid, eutectic, and solid-state/hydrogel electrolytes. A comparative overview of these electrolyte systems, outlining their respective advantages and limitations, is presented in **Table 2**.

Despite these considerable advancements, the low voltage and poor cycling capacity of AZSB are still the bottleneck in battery performance. Therefore, determining the most suitable electrolyte system remains a challenge, as each approach presents its own set of advantages and limitations. Continued interdisciplinary efforts in materials science, electrochemistry, and computational modeling will be key to overcoming existing bottlenecks and advancing AZSB technology toward practical applications. Based on our analysis, it is recommended that future efforts should be directed toward the following perspectives:

1) As long as an aqueous electrolyte is in direct contact with both electrodes, it remains difficult to eliminate the persistent challenges of zinc dendrite growth at the anode and sulfur side reactions at the cathode. Instead of optimizing both the

electrodes separately, a shift toward integrated design strategies is essential. Specifically, the development of novel electrolytes capable of simultaneously regulating interfacial reactions at both electrodes offers a promising path forward. By tailoring the electrolyte to interact synergistically with both the zinc anode and sulfur cathode, it becomes possible to achieve concurrent stabilization, suppress unwanted side reactions, and enhance overall electrochemical performance.

2) Selecting an appropriate cosolvent and redox mediator with high solubility in aqueous media and excellent electrochemical stability is critical for developing a suitable electrolyte for AZSBs. Organic cosolvents with strong Zn^{2+} solvation ability can partially or fully replace H_2O molecules in the solvation structure, effectively tuning Zn^{2+} coordination. This interaction helps exclude water from the inner Helmholtz plane (IHP), thereby suppressing water activity and significantly reducing Zn corrosion, a major issue in aqueous electrolytes. Notably, cosolvents with a high Gutmann DN and dielectric constant (ϵ) exhibit stronger binding affinity toward Zn^{2+} ions and are more likely to undergo controlled reductive decomposition, enabling the formation of stable interphases under electrochemical conditions.^[107–110] Further screening of suitable cosolvent that has the ability to form a stable interfacial layer on the sulfur cathode is desirable, as it can reduce side reactions of the S cathode with electrolyte and improve cathode stability.^[50] On the other hand, redox mediators must exhibit fast and reversible redox kinetics, with redox potentials closely matching the equilibrium potential of the sulfur cathode, to effectively facilitate sulfur redox conversion.^[83] Therefore, the future strategy lies in identifying cosolvents and redox mediators that can suppress parasitic reactions, stabilize both electrodes, and maintain high Zn^{2+} ion transport without compromising the conductivity or increasing the cell resistance.

3) Looking forward, the development of water-in-salt and deep eutectic electrolytes offers promising strategies to expand the ESW and stabilize both the anode and cathode. These electrolyte systems reduce free water activity, which can greatly avoid the side reactions and enable more stable cycling performance. However, DES usually suffers from high viscosity and thereby lower ionic conductivity, which limits their future application. Incorporating a minimal, optimized amount of water to form a water-in-DES system can effectively retain the fundamental characteristics of DESs while substantially accelerating reaction kinetics.

4) Toward rational design of advanced electrolytes, a deep understanding of the electrolyte–electrode interface, ionic

Table 2. Overview of pros and cons of key electrolyte modification strategies in AZSBs.

Electrolyte strategy	Pros	Cons
Aqueous dominant electrolytes	High ionic conductivity, low cost, easy to prepare	Narrow voltage window, hydrogen evolution, dendrite formation
Hybrid/cosolvent systems	Improved stability and voltage window, alter Zn^{2+} solvation structure	Moderate cost, some flammable/volatile components
DES-based electrolytes	Excellent electrochemical stability, easy to synthesize, low-cost, biodegradable	High viscosity, lower conductivity
Solid state/hydrogel electrolytes	Safe, flexible, leakage-free, suppresses dendrites	Drying with time, moderate conductivity, expensive

transport mechanisms, and solvation chemistry is essential to understand before investigating new electrolyte compositions. The reaction mechanism of AZSB is also not fully understood. Previous studies have reported varying mechanisms, with inconsistencies regarding the formation of intermediate species. Therefore, to achieve a deeper and more detailed understanding of Zn–S electrochemistry, advanced *in situ* characterization techniques are essential. *In situ* synchrotron-based X-ray techniques, such as extended X-ray absorption fine structure and X-ray absorption near edge structure, can provide detailed insights into the evolving bonding environment of the cathode during the conversion reactions. Furthermore, dissolved intermediates can be effectively captured and identified using *in situ* techniques such as Raman spectroscopy, nuclear magnetic resonance (NMR), UV-visible spectroscopy, and mass spectrometry (MS).

5) Incorporation of hydrogel-based or quasisolid-state electrolytes can offer benefits of enhanced mechanical stability, suppressed zinc dendrite formation, and reduced electrolyte leakage, thereby contributing to safer and more durable AZSBs.^[27,67,104,105,111]

6) Temperature variations significantly impact battery performance. AZSBs exhibit stable operation primarily at room temperature.^[112–115] However, at low temperatures, the aqueous electrolyte tends to solidify, while at high temperatures, it may boil, which hinders normal functioning. To broaden the operational temperature range of AZSBs, it is crucial to engineer electrolyte compositions with precision. This includes optimizing the arrangement of the tetrahedral structure of H₂O molecules and carefully regulating the interactions among salt components, additives, and the water solvent. To address low-temperature limitations, it is suggested to use antifreezing cosolvents such as EG or glycerol, which can effectively depress the freezing point of the electrolyte.^[49,116] For high-temperature conditions, incorporating high-boiling-point cosolvents can improve the thermal stability of the electrolyte and suppress evaporation. By integrating both antifreezing and heat-resistant cosolvents, a more robust electrolyte system can be developed, ensuring consistent AZSB performance across a wide temperature range.

7) Last but not least, the design and modification of electrolytes for AZSBs must carefully consider the associated costs and, consequently, their scalability. While certain chemicals, whether used as zinc salts, cosolvents, or redox mediator additives, may enhance battery performance, their adoption in real-world applications becomes impractical if the cost is unjustifiable. Hence, a thorough cost–benefit analysis is essential to evaluate the trade-offs between performance gains and economic viability. Future efforts should focus on identifying nontoxic and low-cost chemicals, regardless of their specific role in the electrolyte, projecting AZSB further as a low-cost and environmentally benign energy storage system.

Acknowledgements

All authors thank the Indian Institute of Technology Roorkee, India, for its valuable support. D.P. acknowledges the Government of India for Prime Minister Research Fellowship.

Conflict of Interest

The authors declare no conflict of interest.

Keywords: additives · aqueous zinc–sulfur batteries · electrolytes · solid-electrolyte interfaces

- [1] S. Chen, C. Zhang, X. Lu, *Energy Conversion from Fossil Fuel to Renewable Energy*. In *Handbook of Air Quality and Climate Change*, Springer, Singapore 2023, p. 1.
- [2] M. M. Biswas, M. S. Azim, T. K. Saha, U. Zobayer, M. C. T. Urmi, *Smart Grid Renewable Energy* 2013, 4, 122.
- [3] T. Kim, W. Song, D.-Y. Son, L. K. Ono, Y. Qi, *J. Mater. Chem. A* 2019, 7, 2942.
- [4] H. Dong, J. Li, J. Guo, F. Lai, F. Zhao, Y. Jiao, D. J. L. Brett, T. Liu, G. He, I. P. Parkin, *Adv. Mater.* 2021, 33, 2007548.
- [5] F. Wang, O. Borodin, T. Gao, X. Fan, W. Sun, F. Han, A. Faraone, J. A. Dura, K. Xu, C. H. Wang, *Nat. Mater.* 2018, 17, 543.
- [6] Y. Lv, Y. Xiao, L. Ma, C. Zhi, S. Chen, *Adv. Mater.* 2022, 34, 2106409.
- [7] Y. Zeng, X. F. Lu, S. L. Zhang, D. Luan, S. Li, X. W. Lou, *Angew. Chem. Int. Ed.* 2021, 60, 22189.
- [8] M. Tang, Q. Zhu, P. Hu, L. Jiang, R. Liu, J. Wang, L. Cheng, X. Zhang, W. Chen, H. Wang, *Adv. Funct. Mater.* 2021, 31, 2102011.
- [9] Y. Fu, Q. Wei, G. Zhang, X. Wang, J. Zhang, Y. Hu, D. Wang, L. Zuin, T. Zhou, Y. Wu, S. Sun, *Adv. Energy Mater.* 2018, 8, 1801445.
- [10] M. Liao, J. Wang, L. Ye, H. Sun, Y. Wen, C. Wang, X. Sun, B. Wang, H. Peng, *Angew. Chem.* 2020, 132, 2293.
- [11] L. E. Blanc, D. Kundu, L. F. Nazar, *Joule* 2020, 4, 771.
- [12] Z. Huang, P. Jaumaux, B. Sun, X. Guo, D. Zhou, D. Shanmukaraj, M. Armand, T. Rojo, G. Wang, *Electrochem. Energy Rev.* 2023, 6, 21.
- [13] H. Song, K. Münch, X. Liu, K. Shen, R. Zhang, T. Weintraut, Y. Yusim, D. Jiang, X. Hong, J. Meng, Y. Liu, M. He, Y. Li, P. Henkel, T. Brezesinski, J. Janek, Q. Pang, *Nature* 2025, 637, 846.
- [14] H. Raza, S. Bai, J. Cheng, S. Majumder, H. Zhu, Q. Liu, G. Zheng, X. Li, G. L.-S. Chen, *Achievements and Opportunities*. *Electrochem. Energy Rev.* 2023, 6, 29.
- [15] S. Li, W. Zhang, J. Zheng, M. Lv, H. Song, L. Du, *Adv. Energy Mater.* 2021, 11, 2000779.
- [16] J. Wang, H. Wang, S. Jia, Q. Zhao, Q. Zheng, Y. Ma, T. Ma, X. Li, *J. Energy Storage* 2023, 72, 108372.
- [17] M. Salama, R. AttiasR. Yemini, Y. Gofer, D. Aurbach, M. Noked, *ACS Energy Lett.* 2019, 4, 436.
- [18] M. Zhao, B.-Q. Li, X.-Q. Zhang, J.-Q. Huang, Q. Zhang, *ACS Cent. Sci.* 2020, 6, 1095.
- [19] D. Patel, A. K. Sharma, *Energy Fuels* 2023, 37, 10897.
- [20] T. Bendikov, C. Yarnitzky, S. Licht, *J. Phys. Chem. B* 2002, 106, 2989.
- [21] W. Li, K. Wang, K. Jiang, *Adv. Sci.* 2020, 7, 2000761. <https://doi.org/10.1002/advs.202000761>.
- [22] Y. Guo, R. Chua, Y. Chen, Y. Cai, E. J. J. Tang, J. J. N. Lim, T. H. Tran, V. Verma, M. W. Wong, M. Srinivasan, *Small* 2023, 19, 2207133.
- [23] D. Yuan, J. Zhao, H. Ren, Y. Chen, R. Chua, E. T. J. Jie, Y. Cai, E. Edison, W. ManalastasJr., M. W. Wong, M. Srinivasan, *Angew. Chem.* 2021, 133, 7289.
- [24] D. Yuan, X. Li, H. Yao, Y. Li, X. Zhu, J. Zhao, H. Zhang, Y. Zhang, E. T. J. Jie, Y. Cai, M. Srinivasan, *Adv. Sci.* 2023, 10, 2206469.
- [25] Z. Xu, Y. Zhang, W. Gou, M. Liu, Y. Sun, X. Han, W. Sun, C. Li, *Chem. Commun.* 2022, 58, 8145.
- [26] M. Yang, Z. Yan, J. Xiao, W. Xin, L. Zhang, H. Peng, Y. Geng, J. Li, Y. Wang, L. Liu, Z. Zhu, *Angew. Chem.* 2022, 134, e202212666.
- [27] A. Amiri, K. Bashandeh, R. Sellers, L. Vaught, M. Naraghi, A. A. Polycarpou, *J. Mater. Chem. A* 2023, 11, 10788.
- [28] S. Zhao, X. Wu, J. Zhang, C. Li, Z. Cui, W. Hu, R. Ma, C. Li, *J. Energy Chem.* 2024, 95, 325.
- [29] T. Zhou, H. Wan, M. Liu, Q. Wu, Z. Fan, Y. R. Zhu, *Mater. Today Energy* 2022, 27, 101025.
- [30] W. Wu, S. Wang, L. Lin, H.-Y. Shi, X. Sun, *Energy Environ. Sci.* 2023, 16, 4326.
- [31] P. Hei, Y. Sai, C. Liu, W. Li, J. Wang, X. Sun, Y. Song, X. -X. Liu, *Angew. Chem. Int. Ed.* 2024, 63, e202316082.
- [32] J. Li, J. Liu, F. Xie, R. Bi, L. Zhang, *Angew. Chem.* 2024, 136, e202406126.

- [33] Y. Guo, G. J. H. Lim, V. Verma, Y. Cai, K. K. Chan, E. J. J. Tang, M. Srinivasan, *Chem. Eng. J.* **2024**, *498*, 155329.
- [34] C. Feng, X. Jiang, Q. Zhou, T. Li, Y. Zhao, Z. Niu, Y. Wu, H. Zhou, M. Wang, X. Zhang, M. Chen, L. Ni, G. Diao, Y. Wei, *J. Mater. Chem. A* **2023**, *11*, 18029.
- [35] W. Zhang, M. Wang, J. Ma, H. Zhang, L. Fu, B. Song, S. Lu, K. Lu, *Adv. Funct. Mater.* **2023**, *33*, 2210899.
- [36] P. Peljo, H. H. Girault, *Energy Environ. Sci.* **2018**, *11*, 2306.
- [37] X. Zhao, X. Liang, Y. Li, Q. Chen, M. Chen, *Energy Storage Mater.* **2021**, *42*, 533.
- [38] F. Wan, J. Zhu, S. Huang, Z. Niu, *Batter. Supercaps* **2020**, *3*, 323.
- [39] Y. Yu, J. Xie, H. Zhang, R. Qin, X. Liu, X. Lu, *Small Sci.* **2021**, *1*, 2000066.
- [40] A. Slesinski, S. Sroka, K. Fic, E. Frackowiak, J. Menzel, *ACS Appl. Mater. Interfaces* **2022**, *14*, 37782.
- [41] T. Guo, D. Zhou, L. Pang, S. Sun, T. Zhou, J. Su, *Small* **2022**, *18*, 2106360.
- [42] Y. Liang, M. Qiu, P. Sun, W. Mai, *Adv. Funct. Mater.* **2023**, *33*, 2304878.
- [43] B. Wu, Y. Mu, Z. Li, M. Li, L. Zeng, T. Zhao, *Chin. Chem. Lett.* **2023**, *34*, 107629.
- [44] S. Guo, L. Qin, T. Zhang, M. Zhou, J. Zhou, G. Fang, S. Liang, *Energy Storage Mater.* **2021**, *34*, 545.
- [45] D. Chao, W. Zhou, F. Xie, C. Ye, H. Li, M. Jaroniec, S.-Z. Qiao, *Sci. Adv.* **2020**, *6*, eaba4098.
- [46] X. Li, X. Wang, L. Ma, W. Huang, *Adv. Energy Mater.* **2022**, *12*, 2202068.
- [47] Z. Li, Y. Liao, Y. Wang, J. Cong, H. Ji, Z. Huang, Y. Huang, *Energy Storage Mater.* **2023**, *56*, 174.
- [48] Y. Guo, X. Zhu, J. Zhang, T. Zhang, Z. Wang, M. Shan, F. Wang, C. C. Cao, G. Xu, M. Zhu, *Angew. Chem. Int. Ed.* **2025**, *64*, e202422047.
- [49] S. Mehta, S. Kaur, M. Singh, M. Kumar, K. Kumar, S. K. Meena, T. C. Nagaiah, *Adv. Energy Mater.* **2024**, *14*, 2401515.
- [50] J. Li, J. Cong, Y. Ren, H. Ji, Z. Li, Y. Huang, *Energy Storage Mater.* **2024**, *70*, 103541.
- [51] A. Pei, G. Zheng, F. Shi, Y. Li, Y. Cui, *Nano Lett.* **2017**, *17*, 1132.
- [52] X. Zhou, Y. Lu, Q. Zhang, L. Miao, K. Zhang, Z. Yan, F. Li, J. Chen, *ACS Appl. Mater. Interfaces* **2020**, *12*, 55476.
- [53] J. Shin, J. Lee, Y. Park, J. W. Choi, *Chem. Sci.* **2020**, *11*, 2028.
- [54] Z. Zhao, J. Zhao, Z. Hu, J. Li, J. Li, Y. Zhang, C. Wang, G. Cui, *Energy Environ. Sci.* **2019**, *12*, 1938.
- [55] Y. Geng, L. Pan, Z. Peng, Z. Sun, H. Lin, C. Mao, L. Wang, L. Dai, H. Liu, K. Pan, X. Wu, Q. Zhang, Z. He, *Energy Storage Mater.* **2022**, *51*, 733.
- [56] X. Guo, G. He, *J. Mater. Chem. A* **2023**, *11*, 11987.
- [57] J. Hao, X. Li, S. Zhang, F. Yang, X. Zeng, S. Zhang, G. Bo, C. Wang, Z. Guo, *Adv. Funct. Mater.* **2020**, *30*, 2001263.
- [58] W. Yang, X. Du, J. Zhao, Z. Chen, J. Li, J. Xie, Y. Zhang, Z. Cui, Q. Kong, Z. Zhao, C. Wang, Q. Zhang, G. Cui, *Joule* **2020**, *4*, 1557.
- [59] Y. Yu, W. Xu, X. Liu, X. Lu, *Adv. Sustainable Syst.* **2020**, *4*, 2000082.
- [60] M. A. I. Mohd Shumiri, M. Najib, A. Sani, N. A. C. Fadil, *Sci. Technol. Adv. Mater.* **2025**, *26*, 2448418.
- [61] Y. Liu, X. Lu, F. Lai, T. Liu, P. R. Shearing, I. P. Parkin, G. He, D. J. L. Brett, *Joule* **2021**, *5*, 2845.
- [62] F. E.-T. Heikal, W. R. Abd-Ellatif, N. S. Tantawy, A. A. Taha, *RSC Adv.* **2018**, *8*, 3816.
- [63] S. Chen, H. Wang, M. Zhu, F. You, W. Lin, D. Chan, W. Lin, P. Li, Y. Tang, Y. Zhang, *Nanoscale Horiz.* **2022**, *8*, 29.
- [64] H. Jia, Z. Wang, B. Tawiah, Y. Wang, C.-Y. Chan, B. Fei, F. Pan, *Nano Energy* **2020**, *70*, 104523.
- [65] W. Li, Y. Ma, P. Li, X. Jing, K. Jiang, D. S. Wang, *Adv. Funct. Mater.* **2021**, *31*, 2101237.
- [66] F. Kurnia, J. N. Hart, *ChemPhysChem* **2015**, *16*, 2397.
- [67] H. Zhang, Z. Shang, G. Luo, S. Jiao, R. Cao, Q. Chen, K. Lu, *ACS Nano* **2022**, *16*, 7344.
- [68] M. Yang, Z. Yan, J. Xiao, W. Xin, L. Zhang, H. Peng, Y. Geng, J. Li, Y. Wang, L. Liu, Z. Zhu, *Angew. Chem. Int. Ed.* **2022**, *61*, e202212666.
- [69] J. Liu, C. Ye, H. Wu, M. Jaroniec, S.-Z. Qiao, *J. Am. Chem. Soc.* **2023**, *145*, 5384.
- [70] P. Sun, L. Ma, W. Zhou, M. Qiu, Z. Wang, D. Chao, W. Mai, *Angew. Chem. Int. Ed.* **2021**, *60*, 18247.
- [71] H. Jian, X. Yi, L. Yang, S. Zhang, H. Li, F. Gao, *Langmuir* **2025**, *41*, 7118.
- [72] L. Wang, Y. Zhang, H. Hu, H.-Y. Shi, Y. Song, D. Guo, X.-X. Liu, X. Sun, *ACS Appl. Mater. Interfaces* **2019**, *11*, 42000.
- [73] X. Ji, *eScience* **2021**, *1*, 99.
- [74] C. Sun, R. Miao, J. Li, Y. Sun, Y. Chen, J. Pan, Y. Tang, P. G. Wan, *ACS Appl. Mater. Interfaces* **2023**, *15*, 20089.
- [75] W. Kaveevivitchai, A. Manthiram, *J. Mater. Chem. A* **2016**, *4*, 18737.
- [76] N. Patil, C. de la Cruz, D. Ciurdură, A. Mavrandonakis, J. Palma, R. Marcilla, *Adv. Energy Mater.* **2021**, *11*, 2100939.
- [77] J. Cui, Y. Li, H. Zhang, D. G. Ivey, *Electrochim. Acta* **2025**, *530*, 146418.
- [78] S. Wang, W. Wu, Q. Jiang, C. Li, H.-Y. Shi, X.-X. Liu, X. Sun, *Chem. Sci.* **2025**, *16*, 1802.
- [79] A. Clarisza, H. K. Bezabah, S.-K. Jiang, C.-J. Huang, B. W. Olbasa, S.-H. Wu, W.-N. Su, B. J. Hwang, *ACS Appl. Mater. Interfaces* **2022**, *14*, 36644.
- [80] B. Lee, H. R. Seo, H. R. Lee, C. S. Yoon, J. H. Kim, K. Y. Chung, B. W. Cho, S. H. Oh, *ChemSusChem* **2016**, *9*, 2948.
- [81] Y. Arafat, M. R. Azhar, Y. Zhong, H. R. Abid, M. O. Tadé, Z. Shao, *Adv. Energy Mater.* **2021**, *11*, 2100514.
- [82] M. Cheng, R. Yan, Z. Yang, X. Tao, T. Ma, S. Cao, F. Ran, S. Li, W. Yang, C. Cheng, *Adv. Sci.* **2022**, *9*, 2102217.
- [83] J. Zhou, A. Sun, *Chem. Eng. J.* **2024**, *495*, 153648.
- [84] G. Chang, J. Liu, Y. Hao, C. Huang, Y. Yang, Y. Qian, X. Chen, Q. Tang, A. Hu, *Chem. Eng. J.* **2023**, *457*, 141083.
- [85] Z. Zhao, L. Tian, Q. Bai, R. Pathak, J. Chen, Y. Ye, Y. Wang, J. W. Elam, X. Wang, *Adv. Funct. Mater.* **35**, 250132.
- [86] B. Wanyan, Y. Zhan, Z. Miao, W. Guo, J. Wang, L. Yan, L. Zhang, H. Yu, T.-F. Yi, J. Shu, *Compos. Part B Eng.* **2024**, *284*, 111709.
- [87] H. Yu, Z. Wang, R. Zheng, L. Yan, L. Zhang, J. Shu, *Angew. Chem.* **2023**, *135*, e202308397.
- [88] D. Liu, B. He, Y. Zhong, J. Chen, L. Yuan, Z. Li, Y. Huang, *Nano Energy* **2022**, *101*, 107474.
- [89] C. M. Puzzarini, *J. Phys. Chem. A* **2012**, *116*, 4381.
- [90] S. Shen, C. Yuan, Y. Xu, Y. Xie, L. Wang, T. Yan, S. Chen, L. Wang, T. Liu, L. Zhang, *Adv. Funct. Mater.* **2025**, *35*, 2420258.
- [91] D. Patel, A. Dharmesh, Y. Sharma, P. Rani, A. K. Sharma, *Chem. Eng. J.* **2024**, *479*, 147722.
- [92] T. S. Thomas, A. P. Sinha, D. Mandal, *J. Mater. Chem. A* **2024**, *12*, 21350.
- [93] Z. Ge, H. Liu, S. Wang, Y. Ma, W. Xu, L. Su, L. Han, L. Gong, J. Wang, **2025**, *18*, e202401429.
- [94] G. Yaman Uzunoglu, R. Yüksel, *Small* **2025**, *21*, 2411478.
- [95] J. Wu, Q. Liang, X. Yu, Q.-F. Lü, L. Ma, X. Qin, G. Chen, B. Li, *Adv. Funct. Mater.* **2021**, *31*, 2011102.
- [96] L. Geng, J. Meng, X. Wang, C. Han, K. Han, Z. Xiao, M. Huang, P. Xu, L. Zhang, L. Zhou, L. Mai, *Angew. Chem. Int. Ed.* **2022**, *61*, e202206717.
- [97] C. Zhang, L. Zhang, G. Yu, *Acc. Chem. Res.* **2020**, *53*, 1648.
- [98] X. Hou, T. P. Pollard, X. He, L. Du, X. Ju, W. Zhao, M. Li, J. Wang, E. Paillard, H. Lin, J. Sun, K. Xu, O. Borodin, M. Winter, J. Li, *Adv. Energy Mater.* **2022**, *12*, 2200401.
- [99] R. Chen, C. Zhang, J. Li, Z. Du, F. Guo, W. Zhang, Y. Dai, W. Zong, X. Gao, J. Zhu, Y. Zhao, X. Wang, G. He, *Energy Environ. Sci.* **2023**, *16*, 2540.
- [100] J. Shi, T. Sun, J. Bao, S. Zheng, H. Du, L. Li, X. Yuan, T. Ma, Z. Tao, *Adv. Funct. Mater.* **2021**, *31*, 2102035.
- [101] M. Cui, J. Fei, F. Mo, H. Lei, Y. Huang, *ACS Appl. Mater. Interfaces* **2021**, *13*, 54981.
- [102] Z. Chen, Z. Huang, J. Zhu, D. Li, A. Chen, Z. Wei, Y. Wang, N. Li, C. H. Zhi, *Adv. Mater.* **2024**, *36*, 2402898.
- [103] A. C. Radjendirane, F. M. Sha, S. Ramasamy, R. Rajaram, S. Angaiah, *Energy Technol.* **2024**, *12*, 2401105.
- [104] A. Amiri, R. Sellers, M. Naraghi, A. A. Polycarpou, *ACS Nano* **2023**, *17*, 1217.
- [105] K. K. Sonigara, J. V. Vaghasiya, C. C. Mayorga-Martinez, M. Pumera, *Npj 2D Mater. Appl.* **2023**, *7*, 45.
- [106] M. Wang, H. Zhang, T. Ding, F. Wu, L. Fu, B. Song, P. Cao, K. Lu, *Sci. China Chem.* **2024**, *67*, 1531.
- [107] J. Chen, H. Zhang, M. Fang, C. Ke, S. Liu, J. Wang, *ACS Energy Lett.* **2023**, *8*, 1723.
- [108] S. Chen, Q. Nian, L. Zheng, B.-Q. Xiong, Z. Wang, Y. Shen, X. H. Ren, *J. Mater. Chem. A* **2021**, *9*, 22347.
- [109] R. Yao, Y. Zhao, L. Wang, C. Xiao, F. Kang, C. Zhi, C. Yang, *Energy Environ. Sci.* **2024**, *17*, 3112.
- [110] D. Patel, A. Sharma, A. Choudhary, R. Kaur, K. K. Pant, A. K. Sharma, *Chem. Eng. J.* **2025**, *517*, 164330.
- [111] R. Ma, Z. Xu, X. Wang, *ENERGY Environ. Mater.* **2023**, *6*, e12464.
- [112] H. Wang, Z. Chen, Z. Ji, P. Wang, J. Wang, W. Ling, Y. Huang, *Mater. Today Energy* **2021**, *19*, 100577.

- [113] F. Yue, Z. Tie, S. Deng, S. Wang, M. Yang, Z. Niu, *Angew. Chem. Int. Ed.* **2021**, *60*, 13882.
- [114] Q. Nian, T. Sun, S. Liu, H. Du, X. Ren, Z. Tao, *Chem. Eng. J.* **2021**, *423*, 130253.
- [115] G. Qu, H. Wei, S. Zhao, Y. Yang, X. Zhang, G. Chen, Z. Liu, H. Li, C. Han, *Adv. Mater.* **2024**, *36*, 2400370.
- [116] P. H. R. Silva, V. L. C. Gonçalves, C. J. A. Mota, *Bioresour. Technol.* **2010**, *101*, 6225.
- [117] R. Sharifian, R. M. Wagterveld, I. A. Digdaya, C. Xiang, D. A. Vermaas, *Energy Environ. Sci.* **2021**, *14*, 781.

Manuscript received: June 19, 2025

Revised manuscript received: July 26, 2025

Version of record online:
